Degradation pathways of 1,4-dioxane in biological and advanced oxidation processes

Ahmed Tawfik

National Research Centre, Water Pollution Research Department, Giza 12622, Egypt, emails: tawfik8@hotmail.com, Tawfik_8@yahoo.com

ABSTRACT

1,4-Dioxane is widely used in industry and seriously contaminates the ecosystem due to intentional discharge into water streams. Treatment of water/wastewater containing 1,4-dioxane is greatly growing since, it is listed as a priority pollutant and a hazardous compound for humans and environment. Degradation pathways of 1,4-dioxane in biological and advanced oxidation processes (AOPs) are extensively discussed in this review to identify potential bottlenecks which limit 1,4-dioxane removal processes and possibly allow the identification of the needed treatment approach. Furthermore, the efficiency of hybrid photocatalytic oxidation processes for treatment of wastewater rich 1,4-dioxane is comprehensively performed. During the degradation of 1,4-dioxane, several by-products/intermediates are produced as the consequence of the ring opening of 1,4-dioxane molecules, namely: ethylene glycol, glycolic acid, oxalate anion and formic acid. The efficiency of AOPs for oxidation of 1,4-dioxane is an excellent technology; however, the treatment cost is still quite high. Phytoremediation of water/wastewater containing 1,4-dioxane is a promising approach where conversion of 1,4-dioxane into biomass is performed avoiding severe pollution conditions.

Keywords: 1,4-Dioxane; Advanced oxidation processes; Hybrid photocatalysis; Biodegradation; Phytoremediation

1. Introduction

The properties of 1,4-dioxane are presented in Table 1 and its concentration is quantified using gas chromatography with solid-phase microextraction (SPME-GC) [1]. 1,4-Dioxane is mainly used as a solvent in the manufacturing processes of various industries, that is, pharmaceuticals, polyester, personnel care products, pesticides, magnetic tapes, papers, cotton, textile, adhesives, cosmetics, dyes, oils, waxes, resins, cellulosic esters and ethers [2]. Furthermore, 1,4-dioxane is frequently utilized as a stabilizing agent for chlorinated solvents such as methyl chloroform 1,1,1-trichloroethane (1,1,1-TCA). Less attention has been given to the negative impacts of 1,4-dioxane which is carelessly discharged into sewerage network and/or water bodies resulting in a severe and serious pollution conditions. The contaminated water with 1,4-dioxane causes liver damage, kidney failure and cancer for humans and animals [3]. Moreover, the presence of 1,4-dioxane in the water creates large contaminant plumes which negatively affects drinking water supplies [4,5].

Treatment of water/wastewater containing 1,4-dioxane is greatly growing since it is listed as a priority pollutant and a hazardous compound for humans and environment [6–8]. The fate of 1,4-dioxane in the environment is urgently required [9]. The removal of 1,4-dioxane from water/wastewater using air-stripping and adsorption was quite poor due to its high solubility and low vapor pressure [10]. Distillation at boiling point of 101°C was used for removal of 1,4-dioxane by Priddle and Jackson [5] but it is a highly expensive technique. Likely, classical oxidation processes using chlorine was efficient for elimination of 1,4-dioxane from water/wastewater and unfortunately produced other intermediate compounds more toxic than the original one [7,9,11]. Odah et al. [12] used soil vapor extraction method for removal of

Table 1
1,4-dioxane properties

Formula	Molecular weight	Density	Composition			Boiling point	Heat of vaporization	Freezing point	Specific heat
$C_4H_8O_2$	88.106 Da	1.028 g/cm³	C (54.53%)	H (9.15%)	O (36.32%)	101.2°C	98.6 cal/g	11.85°C	36.01 cal/(mol K)

1,4-dioxane, but a considerable residual value remained in the treated effluent due to a high solubility of the compound which creates preferential partitioning into pore water rather than vapor condition.

Advanced oxidation processes (AOPs) using ozone and hydrogen peroxide ($O_3 + H_2O_2$) [10,13] or H_2O_2 and UV light [13] were efficiently used for removal of 1,4-dioxane from water/wastewater (Table 2). Combination of hydrogen peroxide and ferrous iron [3] rapidly oxidized 1,4-dioxane into more readily biodegradable by-products (Fig. 1). Yamazaki et al. [3] found that addition of Fe(II) under ultrasonic irradiation improved the degradation rate of 1,4-dioxane and mineralization process. 85% and 75% removal of the 1,4-dioxane were achieved in the microwave-generated plasma under alkaline and acidic conditions, respectively, at reaction time of 5 min. The immobilization of gold nanoparticles on titanium dioxide ($Au–TiO_2$) promoted the photocatalytic degradation of 1,4-dioxane [14,15]. However, the cost of applying such technologies is quite high and undoubtedly prohibitive for treatment of wastewater/ water streams containing high concentrations of 1,4-dioxane. Although less economical than biological treatment processes, AOPs could be efficiently used for partial break down of non-biodegradable and/or refractory pollutants into simpler molecules, which can be further biologically biodegraded [16–18].

Unfortunately, biological treatment processes of 1,4-dioxane have not yet emerged as viable alternatives [19–21]. However, some pure culture aerobic microbes efficiently degraded 1,4-dioxane under particular conditions [22–25]. Moving-bed biofilm [7,26], photo-Fenton oxidation coupled with activated sludge process, up-flow biological aerated filter was extensively investigated for treatment of wastewater containing 1,4-dioxane. However, the impact of the presence of chlorinated solvent co-contaminants on biodegradation of 1,4-dioxane needs to be further investigated [27]. DoD SERDP [28] found that monooxygenase-expressing bacteria are very efficient for removal of 1,4-dioxane. The presence of TCA and 1,1-dichloroethene inhibited 1,4-dioxane degradation using bacterial isolates.

2. Advanced oxidation processes

AOPs are extensively used for the degradation of 1,4-dioxane where strong oxidants such as HO• radicals are produced and they play a key role for oxidation process [29]. Fortunately, AOPs can be independently used as a pre- or post-treatment step for oxidation of 1,4-dioxane [30–33]. AOPs use hydroxyl radicals (HO•) to oxidize and sub-sequentially convert 1,4-dioxane into carbon dioxide and water. Table 2 summarizes the operational conditions and efficiency of AOPs for treatment of wastewater containing 1,4-dioxane. Direct single effect of UV photolysis and ozonation was not effective for removal of 1,4-dioxane from water [34,35]. Merayo et al. [36] found that 1,4-dioxane was rapidly oxidized in the presence of hydrogen peroxide (H_2O_2) and ferrous iron ($FeSO_4$). Ozone (O_3) in combination with hydrogen peroxide (H_2O_2) effectively oxidized 1,4-dioxane to be more readily biodegradable products [34]. Stefan and Bolton [13] investigated the degradation and mechanism of removal of 1,4-dioxane using UV/H_2O_2 process and found that formic acid was produced due to the degradation of 1,2-ethanediol diformate (EDDF) with HO• radicals. Ultrasonic irradiation supplemented with Fe(II) improved the decomposition rate and mineralization efficiency of 1,4-dioxane [37]. Heterogeneous photocatalysis is a promising alternative AOP which comprises a semiconductor catalyst in a solid form (TiO_2, ZnO) incorporated with ultraviolet light (UV) (Fig. 2) [38]. This technique promotes the production of hydroxyl radicals and positive holes on the catalyst surface with a high oxidizing power of ~3.0 eV [39] for degradation of refractory pollutants [40].

2.1. Homogeneous processes

Hydrogen peroxide (H_2O_2) + UV light, $H_2O_2 + O_3$ and H_2O_2 + UV light + O_3 represented the main photochemical homogenous oxidation processes utilized for degradation of 1,4-dioxane rich wastewater (Fig. 3). Furthermore, Fenton process is the electron transfer between H_2O_2 and ferrous ion (Fe^{2+}), which is suitable for treatment of heavily loaded industrial effluents (Fig. 4). Combination of UV light and Fenton reaction process is namely photo-Fenton reaction process where the photo-recovery of catalytic Fe^{2+} and the photo-decarboxylation of the refractory ferric carboxylate complexes took place.

2.1.1. Photochemical

2.1.1.1. UV-photolysis

The degradation of 1,4-dioxane by HO• radicals occurred at wavelengths ≥ 235 nm where these oxidants are produced due to photolysis of H_2O (Eq. (1)) [41–50] (Table 3). The oxidation of 1,4-dioxane using HO• radicals is taken place with UV-C wavelength ranging from 200 to 280 nm, which indicates that 1,4-dioxane is initially degraded by photons (hν) in the UV-A range (Table 2). Both HO• radicals and photons contributed to the degradation process in the photolytic reaction of 1,4-dioxane using UV-C. Coleman et al. [30] found that 1,4-dioxane removal was increased at increasing concentration of HO• radical. However, the removal efficiency of 1,4-dioxane was only 3%–4% under UV-A condition, and slightly increased up to 5%–12% at UV-C of 16.9 mW/cm at reaction time of 4.0 h [41] (Table 2). This was not the case

Table 2
Advanced oxidation processes (AOPs) treating wastewater rich 1,4-dioxane

Processes	Operating conditions	%R	Intermediates	References
1. Homogeneous				
1.1. Photochemical processes				
UV-light	Reaction time (90 min.)	18% as COD		[34]
UV-A region	4.0 h, initial pH of 3	3%–4%		[41–42]
UV-A	Irradiation period (2 h)	<15%		[15]
UV-C region	4.2 m Wcm^{-2}, 4.0 h. initial pH of 3	5%–12%		
O_3/UV	Reaction time (90 min), 1,4-dioxane initial concentration = 100 mg/L	52% as COD		[34]
O_3/H_2O_2/UV	Reaction time (90 min.) 1,4-dioxane initial concentration = 100 mg/L), H_2O_2/O_3 (w/w) = 0.5	94%		[42]
	(pH = 4 and reaction time 90 min) 1,4-dioxane initial concentration = 100 mg/L), H_2O_2/O_3 = 0.5	91%		
	(pH = 7 and reaction time 90 min) 1,4-dioxane initial concentration = 100 mg/L), H_2O_2/O_3 = 0.5	92%		
	(pH = 10 and reaction time 90 min.) 1,4-dioxane initial concentration = 100 mg/L), H_2O_2/O_3 = 0.5	96%		
	(pH = 10 and reaction time 90 min) 1,4-dioxane initial concentration = 100 mg/L), H_2O_2/O_3 = 0.25	92%		
	(pH = 10 and reaction time 90 min) 1,4-dioxane initial concentration = 100 mg/L), H_2O_2/O_3 = 0.75	94%		
	pH = 10 and reaction time 90 min) 1,4-dioxane initial concentration = 100 mg/L), H_2O_2/O_3 = 1	86%		
	pH = 10 and reaction time 90 min.) 1,4-dioxane initial concentration = 100 mg/L), H_2O_2/O_3 = 1.25	75%		
	pH = 10 and reaction time 90 min.) 1,4-dioxane initial concentration = 100 mg/L), H_2O_2/O_3 = 1.5	64%		
1.2. Chemical processes				
Ozone (O_3)	Reaction time (90 min)	35% as COD		[41,42]
	pH > 9, T = 25°C, 1,4-dioxane (247.8 mg/L; 450 mg/L COD_0), 1 g/L (COD) = 2.125 g/L H_2O_2	100%	Ethylene glycol as a primary intermediate at alkaline pH and ethylene glycol diformate at pH of 5.7	[42]
	pH < 5.7, T = 25°C, 1,4-dioxane (247.8 mg/L; 450 mg/L COD_0), 1 g/L COD = 2.125 g/L H_2O_2	100%	pH < 5.7, T = 25°C, 1,4-dioxane (247.8 mg/L; 450 mg/L COD_0), 1 g/L COD = 2.125 g/L H_2O_2	

Table 2 Continued

Processes	Operating conditions	%R	Intermediates	References
Fenton process ($Fe^{2+} + H_2O_2$)	pH = 2.8, $[H_2O_2]_0/COD_0$ = 4.250 and $[H_2O_2]_0/[Fe^{2+}]_0$ = 1)	100%	Ethylene glycol, glycolic acid, oxalate anion and formic acid	[36]
	Initial pH (2.8) with 1M H_2SO_4, optimum molar ratio $[H_2O_2]/[Fe^{2+}]$ = 5, H_2O_2 (35% w/v), $[H_2O_2]_0/[COD]_0$ = 2.125	75% as TOC	Ethylene glycol and formic acid	[43]
2. Heterogeneous				
2.1. Photochemical process				
Zero-valent iron (Fe^0) and UV-C light	4.0 h, 4.2 $mWcm^{-2}$, 5 mg Fe^0/L, initial pH of 3	34%		[41]
Fe^0 and UV-A region	4.0 h, 16.9 $mWcm^{-2}$, 5 mg Fe^0/L, initial pH of 3	89%		
	2.1 $mWcm^{-2}$, initial pH of 3	29%		
Fe^0/UV/ H_2O_2	(1,000 mg $NaHCO_3$/L), (pH 8.5), optimum molar ratio $[H_2O_2]/[Fe^0]$ = 60, H_2O_2 (35% w/v), $[H_2O_2]_0/[COD]_0$ = 2.125, T = 25°C), (Lamp of 450 W), light intensity = 788 Wm^{-2})	100%	Methoxyacetic and acetic acids, Ethylene glycol and formic acid (the main initial by-product). Carboxylic acids was detected.	[43]
Fe^0/solar light/ H_2O_2		65%	EGDF (≤1.1 ± 0.1 mg/L)	[44]
2.2. Chemical				
TiO_2 alone (dark conditions)	No light	0%		[15]
2.3. Photocatalysis				
TiO_2 slurry P25 + UVA	Initial concentration of 1,4-dioxane = 36 ppm, 50 mg/L TiO_2, pH values 3, 7 and 11. Time = 3.0 min	100%	EGDF was detected at both pH 3 and 7, but no EGDF was detected at pH 11	[15]
TiO_2 - sol–gel + UVA	Initial concentration of 1,4-dioxane = 36 ppm, 50 mg/L TiO_2; pH 3 (acidic), pH 7 (neutral), 60 min and 45 min		The reaction was faster as follows, the P25 slurry > P25 immobilised > TiO_2 sol–gel. However, the use of suspension catalyst requires a subsequent filtration step to remove TiO_2 particles from water which certainly increased the treatment cost	
TiO_2 Immobilized P25 + UVA	Initial concentration of 1,4-dioxane = 36 ppm			
TiO_2 + UV		59.0 –87.6%	1,2-ethanediol diformate and formic acid	[3]
	pH 5.0 and 1.5 g/L TiO_2, 0.29 min.	77%		[45]
	(P25-TiO_2 suspension = 10.0 g/L, The initial pH = ≈5.7, T = 25°C), (Lamp of 450 W), light intensity = 788 Wm^{-2}), 360 kJ/L	45%	Ethylene glycol diformate (EGDF) and formic acid. Some acetic acid was detected. The mixture of methoxyacetic and glycolic acids was below 5.6 ± 0.2 mg/L). Ethylene glycol monoformate (EGMF) was ≤0.03 ± 0.01 mg/L	[43]
Solar light/TiO_2	Xe lamp (300 W), light intensity (444 Wm^{-2}), 360 kJ/L, The initial pH = ≈5.7, P25-TiO_2 suspension =10.0 g/L,	45%	EGDF and formic acid	
Solar light/TiO_2	Xe lamp (300 W), light intensity (444 Wm^{-2}), 470 kJ/L	60%		

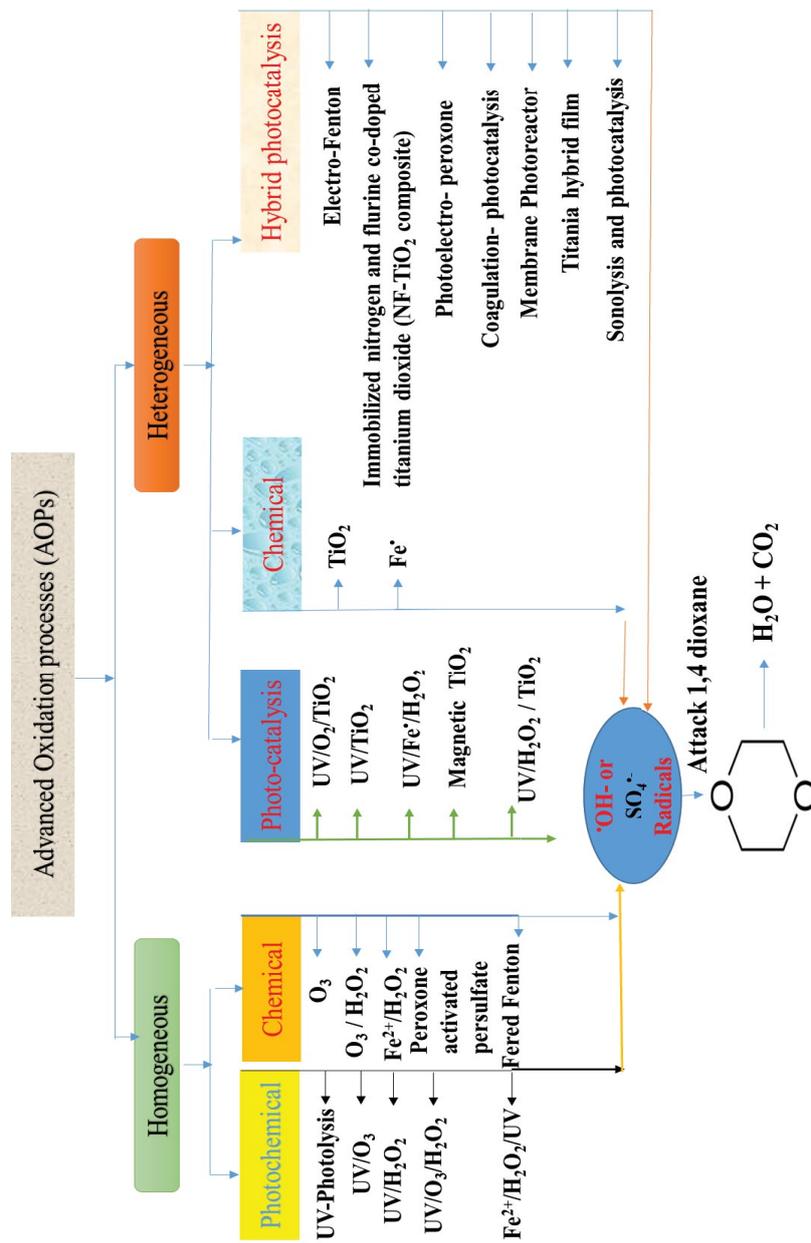|				
TiO_2 + oxygen + UVA/UVB	Light (A > 300 nm) and TiO_2 0.4 g P25 TiO_2	100%	Ethylene glycol diformate (EGDF) (1,2-ethanediol diformate) was the intermediate	[46]
2.4. Hybrid photocatalysis Immobilized nitrogen and fluorine co-doped titanium dioxide (NF-TiO_2) composite with monodisperse TiO_2 nanoparticles	1,4-dioxane (135–140 mg/L), pH 6.9	≤100%	Ethylene glycol diformate (EGDF), ethylene glycol monoformate (EGMF), and formic acid were the major reaction intermediates	[43]
Immobilization of gold nanoparticles on the surface of TiO_2 powder		60%		[47]
TiO_2–$Cs_{2.5}H_{0.5}$–$PW_{12}O_{40}$ hybrid films	4 h of UV radiation	30%		[48]

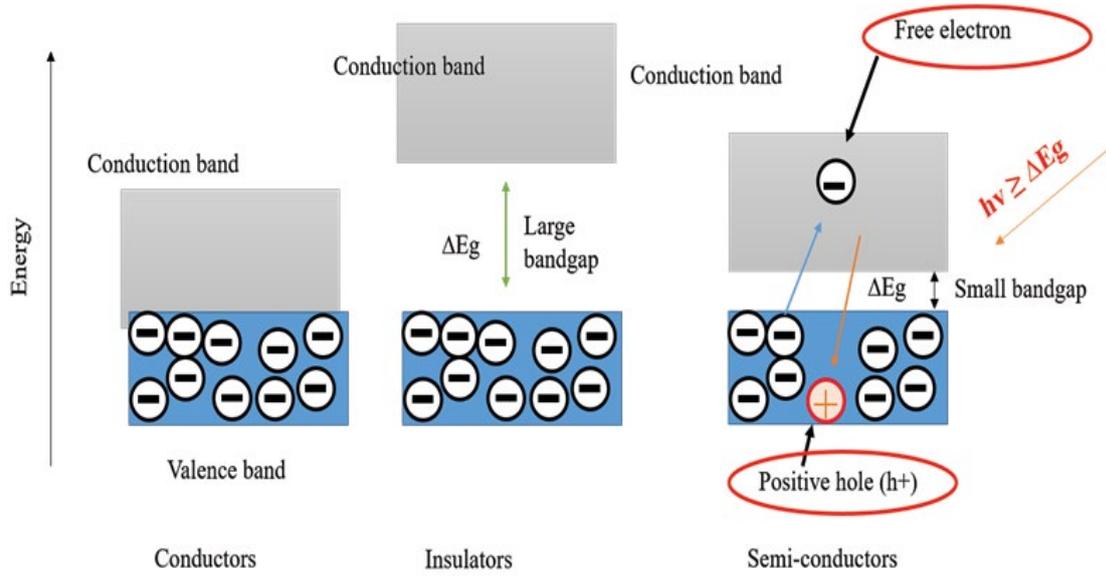Fig. 1. Advanced oxidation processes (AOPs) treating wastewater rich 1,4-dioxane.

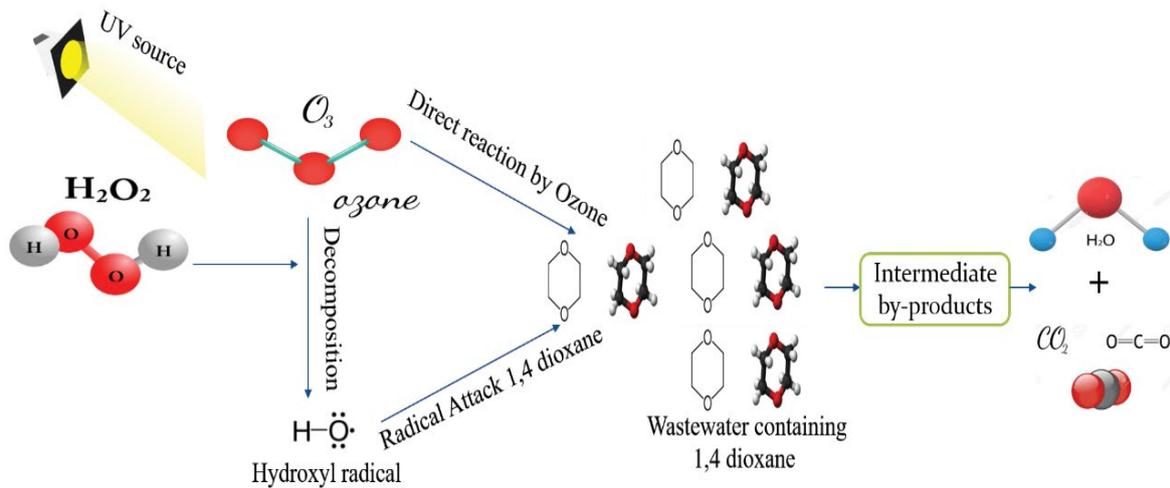Fig. 2. Semiconductor for photocatalysis process.

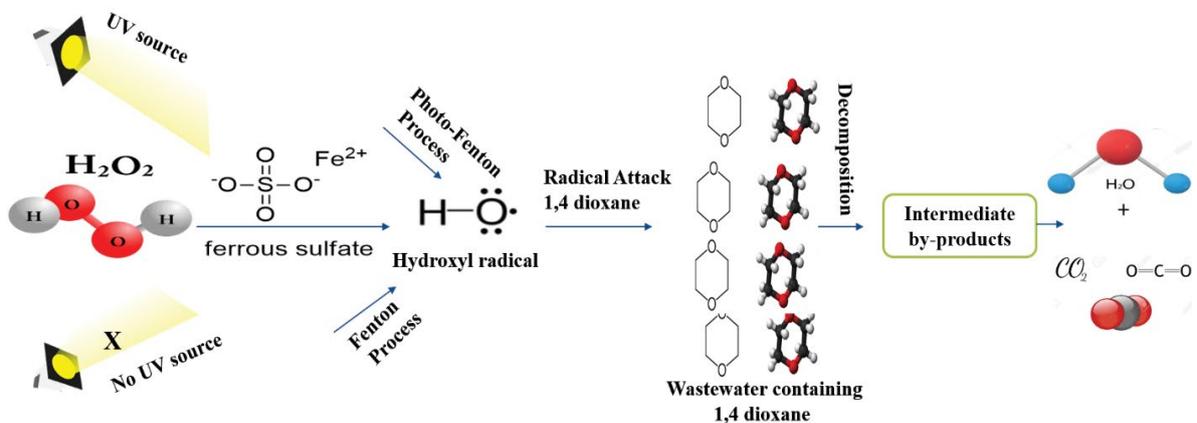Fig. 3. Homogenous oxidation processes degrading 1,4-dioxane rich wastewater.

Fig. 4. Fenton and photoFenton oxidation processes degrading 1,4-dioxane rich wastewater.

for Stefan and Bolton [13] who reported that 1,4-dioxane is a very weak absorber of UV light and subsequently cannot be degraded by photolysis process.

2.1.1.2. UV/hydrogen peroxide (H_2O_2)

Photo-induced oxidation process using UV light in combination with H_2O_2 have proven to be very efficient for the removal of toxic organic pollutants particularly 1,4-dioxane [31–34,51–68]. The degradation of 1,4-dioxane was improved using UV photolysis in the presence of H_2O_2 [69]. 88%–94% removal of the initial concentration of 1,4-dioxane was occurred after 60 min of irradiation. The H_2O_2 generates hydroxyl radical due to photolysis process and rapidly decay of 1,4-dioxane (Eqs. (2) and (3)) into intermediates and finally into carbon dioxide [50,68]. The removal efficiency of 1,4-dioxane was 36.3% using H_2O_2/UV at reaction time of 8.0 h and initial concentration of 450–600 ppm [49] (Table 2). The degradation rate of 1,4-dioxane was optimized at H_2O_2 concentration of 30 ppm resulting in the highest mineralization rate of 0.5 μgC/min. [31] (Table 2). However the mineralization rate was substantially dropped at H_2O_2 concentration of 60 ppm. This was mainly due to an excess of H_2O_2 in the reaction medium that acts as a hydroxyl radical scavenger resulting in a decrease in the mineralization rate of 1,4-dioxane [69]. Excessive addition of H_2O_2 in the reaction medium generates more HO• radicals which will produce much less reactive hydroperoxyl radicals, HOO• [70]. The required concentration of H_2O_2 is mainly dependent on the H_2O_2/1,4-dioxane molar ratio [71].

2.1.1.3. UV/peroxydisulfate ($S_2O_8^{2-}$)

Light assisted degradation of 1,4-dioxane was carried out by Maurino et al. [68] in the presence of sodium peroxydisulfate. The $S_2O_8^{2-}$/UV treatment provided the highest removal efficacy of 1,4-dioxane and total organic carbon (TOC) at wavelength light < 295 nm. Combination of UV irradiation with $S_2O_8^{2-}$ induces a photolytic decomposition resulting in the anion $SO_4^{•2-}$, radical which reacts primarily with the organics as electron acceptor [72]. The $SO_4^{•2-}$ radical is released due to dissociation of peroxydisulfate ($S_2O_8^{2-}$) in the presence of light where organics reacts with $SO_4^{•2-}$ radical according to Eqs. (4)–(6) (Table 3). However Maurino et al. [68] observed a strong inhibition of the $S_2O_8^{2-}$/UV treating 1,4-dioxane in the presence of HCO_3^- where the oxidizing species were scavenged by HCO_3^- resulting in $CO_3^{•}$ [73]. The degradation rate of 1,4-dioxane [RH_2] was decreased due to consumption of HO• and $SO_4^{•2-}$ radicals based on Eqs. (7)–(9) (Table 3). Likely, the photocatalytic degradation of trichloroethylene was inhibited due to the presence of high concentration of bicarbonate ions in the reaction medium [74].

2.1.2. Chemical

2.1.2.1. Ozonation (O_3)

Among the different AOPs, ozone (O_3) is particularly promising oxidizing agent for treatment of recalcitrant organics such as 1,4-dioxane where it has the capability to produce high levels of HO• and the possibility of treating large volume of water flows at full scale [51–55]. O_3 process is very efficient for removal of several toxic non-biodegradable compounds without producing residuals [56–60]. HO• produced through the O_3 decomposition [61–64] is much stronger and less selective oxidant than ozone [65,66]. The O_3 does not react strongly with the 1,4-dioxane compound (Eqs. (10)–(12)) (Table 3) and the removal efficiency is mainly due to oxidation by OH• radicals (Eq. (13)) [67] at alkaline pH value [55,60,64]. This chain reactions of OH• production is initiated in the absence of H_2O_2, by hydroxide anions at high pH values (Eqs. (10) and (11)), where at the reactions proceeds over the conversion of $O_3^{•-}$ into OH• (Eqs. (12) and (13)) (Table 3). Barndok [75] found that ozonation (O_3) of both synthetic solution of 1,4-dioxane and industrial wastewaters containing 1,4-dioxane and 2-methyl-1,3-dioxolane (MDO) was very efficient resulting in 90% of COD removal and complete removal of 1,4-dioxane and MDO. The degradation at pH > 9 occurred faster through the formation of ethylene glycol as a primary intermediate; whereas the decomposition in acidic conditions (pH < 5.7) consisted in the formation and slower degradation of ethylene glycol diformate (Table 3).

2.1.2.2. Peroxone ($H_2O_2 + O_3$)

O_3 plays a crucial role for the release of OH• from H_2O_2 (Eq. (14)) (Table 3). Combination of O_3 with H_2O_2 would accelerate the oxidation process of 1,4-dioxane; however, the use of H_2O_2 can be costly for high loads [11]. The presence of H_2O_2 significantly enhanced the oxidation process of 1,4-dioxane at neutral pH value of 7.0 ± 0.1, as the H_2O_2 contributes to the generation of OH• through adduct formation proceeded by the conversion of $O_3^{•-}$ into HO• radicals [11] (Table 2). The O_3/H_2O_2 process was used to enhance the biodegradability of 1,4-dioxane [11]. Kwon et al. [34] compared the efficiency of O_3, O_3/ultraviolet (UV), and O_3/UV/H_2O_2 for treatment of dioxane-contaminated water and found that the combination H_2O_2/O_3 was efficient for oxidation of 1,4-dioxane and produced more readily biodegradable by-products [11]. The oxidation potential (E_0) of the HO• is 2.80 V which is much higher than those for ozone ($E_0 = 2.07$ V). Combination of ozone with UV and/or H_2O_2 produces hydroxyl, peroxyl and superoxide radicals which should synergistically accelerate the degradation of the organic contaminants [76] (Table 2). HO• radicals are generated due to the interaction between the ozone and the hydrogen peroxide (Eq. (14); Table 3) [77–81]. Complete mineralization of 1,4-dioxane was achieved at H_2O_2/O_3 (w/w) ratio of 0.5 [34]. However, an excess amount of H_2O_2/O_3 (0.75, 1, 1.25 and 1.5) negatively affected on the removal efficiency of 1,4-dioxane which acts as a radical scavenger at high concentrations and the formation of much less powerful •OH_2 radicals (Eq. (15)). Nevertheless, the removal efficiency of 1,4-dioxane was slightly higher at pH 10 (96%) than those achieved at pH 4 (92%) and pH 7 (92%) after reaction time of 90 min. this was mainly due to the highest generation of OH radical (Table 2).

2.1.2.3. Peroxone activated persulfate

Dissolved ozone and hydrogen peroxide were used to activate sodium persulfate resulting in peroxone activated persulfate (PAP) which represents an excellent oxidant for

Table 3
Advanced oxidation reaction mechanisms

Reaction process	Equations		References
1. Homogeneous processes			
1.1. Photochemical reaction			
UV/H_2O_2	$H_2O/OH^- + h\nu \geq 235$ nm $\rightarrow HO^\bullet + H^\bullet$	1	[49,50]
	$H_2O_2 + h\nu (\geq 235$ nm$) \rightarrow 2HO^\bullet$	2	[31–34,
	$C_4H_8O_2 + HO^\bullet \rightarrow C_4H_7O_2^\bullet + H_2O$	3	51–68]
UV/$S_2O_8^{2-}$	$S_2O_8^{2-} + h\nu \rightarrow 2\ SO_4^{\bullet-}$	4	[72–75]
	$SO_4^{\bullet-} + RH_2 \rightarrow SO_4^{2-} + H^+ + RH^\bullet$	5	
	$RH^\bullet + S_2O_8^{2-} \rightarrow R + SO_4^{2-} + H^+ + SO_4^{\bullet-}$	6	
	$CO_3^{\bullet-} + RH_2 \rightarrow HCO_3^- + RH^\bullet$	7	
	$SO_4^{\bullet-} + RH_2 \rightarrow SO_4^{2-} + H^+ + RH^\bullet$	8	
	$OH^\bullet + RH_2 \rightarrow H_2O + RH^\bullet$	9	
1.2. Chemical reactions			
Ozonation (O_3)	$O_3 + OH^- \rightarrow O_2^{\bullet-} + HO_2^\bullet$	10	[56–66]
	$O_3 + O_2^{\bullet-} \rightarrow O_3^{\bullet-} + O_2$	11	
	$O_3^{\bullet-} \rightleftharpoons O^{\bullet-} + O_2$	12	
	$O^{\bullet-} + H_2O \rightleftharpoons OH^\bullet + OH^-$	13	
Peroxone process ($H_2O_2 + O_3$)	$O_3 + H_2O_2 \rightarrow HO^\bullet + HO_2^\bullet + 2O_2$	14	[11,34]
	$^\bullet OH + H_2O_2 \rightarrow HO_2 + H_2O$	15	
Fenton and Fered-Fenton	$Fe^{2+} + H_2O_2 \rightarrow Fe^{3+} + OH^\bullet + OH^-$	16	[111–117]
	$Fe^{3+} + e^- \rightarrow Fe^{2+}\ E^0 = 0.77$ V	17	
	$O_2 + 2H^+ + 2e^- \rightarrow H_2O_2\ E^0 = 0.70$ V	18	
	$2H^+ + 2e^- \rightarrow H_2\ E^0 = 0.0$ V	19	
	$H_2O_2 + 2H^+ + 2e^- \rightarrow 2H_2O\ E^0 = 0.53$V	20	
	Mechanism of H_2O_2 decomposition		
	$Fe^{3+} + H_2O_2 \rightarrow Fe^{2+} + HO_2^\bullet + H^+$	21	
	$Fe^{2+} + OH^\bullet \rightarrow Fe^{3+} + OH^-$	22	
	$Fe^{2+} + HO_2^\bullet \rightarrow Fe^{3+} + HO_2^-$	23	
	$Fe^{3+} + HO_2^\bullet \rightarrow Fe^{2+} + O_2 + H^+$	24	
	$OH^\bullet + H_2O_2 \rightarrow HO_2^\bullet + H_2O$	25	
	$HO_2^\bullet + HO_2^\bullet \rightarrow H_2O_2$	26	
2. Heterogeneous processes			
2.1. Photocatalysis			
Zero-valent iron (Fe^0) microspheres	$Fe^0 + h\nu \rightarrow Fe^{2+} + 2e^-$	27	[43,118–
	$Fe^{2+} + H_2O_2 \rightarrow Fe^{3+} + OH^\bullet + OH^-$	28	121]
	$2H_2O + h\nu (<698$ nm$) \rightarrow HO_2^\bullet + 3H^+$	29	
	$Fe^{2+} + HO_2^\bullet (O_2^{-\bullet}) \rightarrow Fe^{3+} + H_2$	30	
	$HO_2^\bullet (O_2^{-\bullet}) + H \rightarrow H_2O_2 + H_2$	31	
2.2. Hybrid photocatalysis			
Photoelectro-peroxone (PEP) process	$O_2 + 2H^+ + 2e^- \rightarrow H_2O_2$	32	[139–147]
	$2HO_2^- + 2O_3 + H_2O \rightarrow 2OH^- + 3O_2 + HO_2^\bullet + {}^\bullet OH$	33	
	$H_2O_2 + h\nu \rightarrow 2\ {}^\bullet OH$	34	
	$O_3 + H_2O + h\nu \rightarrow 2\ {}^\bullet OH + O_2$	35	

refractory compounds [82]. PAP facilitates the production of two strong oxidants, that is, hydroxyl (2.8 V) and sulfate (2.5 V) radicals for oxidation of organic contaminants [82–84]. PAP was used for in situ remediation and treating of 1,4-dioxane [85–91]. Eberle et al. [91] investigated the fate of single-contaminant of 1,4-dioxane and in the presence of trichloroethene (TCE), and 1,1,1-trichloroethane (1,1,1-TCA) using a peroxone activated persulfate (PAP). They found that the oxidation rate of each contaminant was linearly increased at increasing persulfate concentration and the degradation

rate was in the following order, TCE > 1,4-dioxane > 1,1,1-TCA. Oxidation rates of 1,4-dioxane were 87% slower in the presence of VOCs (Table 2). This is mainly because most of the oxidative radicals were consumed for destruction of VOCs.

2.1.2.4. Fenton (Fe^{2+}/H_2O_2) vs. photo-Fenton ($Fe^{2+}/H_2O_2/UV$)

Fenton process is the most commonly used AOP for conversion of persistent compounds into simple biodegradable substances. It is mainly based on the electron transfer between H_2O_2 and ferrous ion (Fe^{2+}), which represents as a homogenous catalyst for production of HO• radicals to degrade organic compounds [92]. Application of Fenton process for wastewater treatment is relatively limited due to production of iron sludge [93], and the optimal acidic pH values (pH≈3) [94,95]. However iron precipitation as $Fe(OH)_3$ is avoided under acid conditions due to increasing the solubility of iron [96]. Moreover, hydrogen peroxide decomposition is impeded at acidic pH values [97] and the scavenger of inorganic carbon is avoided. Treatment of 1,4-dioxane by Fenton's reagent was extensively investigated by Ghosh et al. [31], Kim et al. [98], Khan et al. [99]. Complete removal of 1,4-dioxane and 80% reduction of the chemical oxygen demand (COD) was achieved by Merayo et al. [36] using Fenton process at pH value of 2.8, initial H_2O_2/COD ratio of 4.25 and H_2O_2/Fe^{2+} ratio of 1. Combination of UV light and Fenton reaction process is namely photo-Fenton process where the photo-recovery of catalytic Fe^{2+} and the photo-decarboxylation of the refractory ferric carboxylate complexes taken place [100–106]. The main drawback of Fenton and photo-Fenton reactions is the acidic pH (3) and production of iron sludge [94,107,108]. Radiation has a significant contribution for enhancement and activation of the Fe^{2+} for removal of 1,4-dioxane [91]. The degradation efficiency of 1,4-dioxane was increased from 36.3% to 52% in case of adding 2,800 ppm of both H_2O_2 and $FeSO_4$ in the photo-Fenton oxidation process [107,108] (Table 2). This is mainly due to an increase of HO• in the presence of light.

2.1.2.5. Fered-Fenton

Degradation of 1,4-dioxane using Fenton oxidation process (Eq. (16)) mainly occurred at long reaction time [109]. This is mainly due to the low reduction rate of Fe^{3+} into Fe^{2+} (Eq. (17)). Likely, photo-Fenton utilizes UV irradiation in combination with the Fenton reaction process for reduction of ferric ions [98,110]. Ferrioxalate-mediated photo-Fenton process was also used to increase the reduction rate of Fe^{3+} [111]. Recently, electro-Fenton has received a great attention for degradation of various organic pollutants [112–114]. A portion of the Fenton reagent is fortunately generated in situ in an electrochemical cell particularly at the cathode (Eqs. (17) and (18)) (Table 3). Fe^{3+} reduction occurred (Eq. (17)) and H_2O_2 is formed due to a reduction of dissolved oxygen (Eq. (18)). Reactions (Eqs. (19) and (20)) took place as side reactions. Combination of electro-Fenton with H_2O_2 namely Fered-Fenton process (Eqs. (16) (21)–(26)) (Table 2) has been investigated earlier in the literature [115,116] for the degradation of organic pollutants as well as for removal of 1,4-dioxane [117]. Addition of H_2O_2 enhanced the release of HO• radicals for complete degradation of 1,4-dioxane. The authors used activated carbon sheet as a cathodic electrode and the residual values of 1,4-dioxane was quite low (0.5 mg/L) at influent concentrations of 40 and 100 mg/L.

2.2. Heterogeneous processes

Incomplete chemical oxidation of 1,4-dioxane using chlorine (NaClO) and Fenton's reagent was reported by Klečka and Gonsior [109]. H_2O_2 and 1,4-dioxane are very weak absorbers of UV light. Approximately 50.8% and 0.15% of the UV light entering the reactor is absorbed by H_2O_2 and 1,4-dioxane, respectively. Photocatalysis is the combination of UV light and semiconductor catalyst, that is, TiO_2, ZnO where minimal production of residues and mild operation conditions for wastewater treatment is attained. The use of zero valent iron (Fe•) instead of Fe^{2+} salts at neutral pH and moderate carbonaceous alkalinity overcome the drawbacks of classical photo-Fenton process. The produced Fe^{2+} remains anchored on the surface of Fe• microspheres during heterogeneous process avoiding generation of iron sludge. Moreover, UV/TiO_2 oxidation of 1,4-dioxane under alkaline pH conditions promoted the hydrolysis of EGDF to EG [68]. The disappearance of oxalic acid indicated that the reaction reached a stage where complete mineralization of the 1,4-dioxane took place [13–36].

2.2.1. Photocatalysis

2.2.1.1. Zero-valent iron (Fe^0) microspheres

Zero-valent iron (Fe^0) is necessary for microorganisms to carry out the oxidation and degradation of dissolved organics [118]. The free electrons are generated from Fe^0 and play a role as a reductant for other materials due to the oxidation–reduction process between Fe^{2+} and Fe^{3+} ions [119]. Fe^0 was used as a reducing agent for the degradation of pollutants [120,121]. Furthermore, there is no problem for light penetration using Fe^0 where the turbidity is not increased during the reaction and it is easy to activate it. The degradation of 1,4-dioxane using only zero-valent iron (Fe^0), photolysis and combined Fe^0 with UV light was investigated by Son et al. [41]. They found that the degradation rate constant (19×10^{-4}/min), in the combined reaction (5 mg/L Fe^0/4.2 mW/cm UV-C light) was higher than those obtained for Fe^0-only (4.8×10^{-4}/min) and photolytic reactions (2.25×10^{-4}/min), respectively (Table 2). The oxidation process using Fe^0 is preferable for pollutants removal using Fenton reaction process (Eqs. (27) and (28)) (Table 3). The removal of 1,4-dioxane in the presence of Fe^0-only and combined reactions might be due to the adsorption and oxidation reaction. Adsorption and surface reaction are the two basic mechanisms for 1,4-dioxane removal using Fe^0. The bonding energy between Fe^0 and 1,4-dioxane decreased by adding UV and the adsorption and desorption degrees of 1,4-dioxane on Fe^0 surface changed by UV irradiation. 1,4-dioxane was mostly degraded by OH• radicals in the combined reaction and was fitted well to the Langmuir–Hinshelwood model, indicating that adsorption as well as the chemical reaction was the main removal mechanism. The transformation of Fe^0 into Fe^{2+} and Fe^{3+} was observed in the combined reactions (Fe^0 with UV) and the conversion rate of Fe^0 was substantially improved by

UV irradiation (Eqs. (27) and (28)) (Table 3). However, the removal of 1,4-dioxane using Fe^0 is UV source dependent where UV light can be used as the energy source for the oxidation of Fe^0 and for generation of H_2O_2. The removal efficiency of 1,4-dioxane in combined reaction (Fe^0 and UV-C) at reaction time of 4.0 h, was quite higher (34% at 4.2 mW/cm^2 and 89% at 16.9 mW/cm^2) as compared with Fe^0 and UV-A (29% at 2.1 mW/cm^2, and 33% at 12.6 mW/cm^2) [43,44] (Table 2). Moreover, Bielski et al. [122], Balmer and Sulzberger, [123], Jeong and Joon [124] showed that H_2O_2 can be produced by the $OH_2^{\bullet}$ radical, which is formed from the photolysis of H_2O at wave length < 698 nm (Eqs. (29)–(31)) (Table 3). Oxidation of Fe^0 by UV produces Fe^{2+}, which reacts with $OH_2^{\bullet}$ to form Fe^{3+} and H_2O_2 allowing a Fenton-like reaction without supplementation of H_2O_2. Complete removal of 1,4-dioxane and 85% removal of TOC were achieved by Barndõk et al. [44] using Fe^0/UV radiation (60 kJ/L) and was dropped to 95% at artificial UV radiation of 20 kJ/L (Table 2). Fe^0/H_2O_2/solar process provided 65% removal of 1,4-dioxane with the consumption rate of 480 kJ/L (Table 2). Ethylene glycol and formic acid were dominant reaction intermediates using Fe^0/H_2O_2/UV process [43]. Methoxyacetic and glycolic acids were produced at the beginning of the reaction, resulting in maximum concentrations at contact time of 60 min which was slowly degraded afterwards. Acetic and oxalic acids appeared after 60 min. and accumulated to a lesser extent during the reaction process (Table 2).

2.2.1.2. Titanium dioxide (TiO$_2$)

The use of TiO$_2$ photocatalysts (Fig. 5) for treatment of wastewater containing refractory and non-biodegradable organics has recently gained a great of interest. TiO$_2$ is stable, harmless, inexpensive and can be easily activated by solar energy and reused [125–127]. No removal of 1,4-dioxane was observed using titanium dioxide under dark conditions [15]. Hill et al. [46] found that 1,4-dioxane is readily oxidized in the presence of oxygen, UVA/UVB and titanium dioxide as catalyst. However, toxic intermediates were produced from photo-oxidation of 1,4-dioxane, that is, ethylene diformate [46,68]. Several researchers [46,68] investigated photocatalytic degradation and reaction pathway of wastewater rich in 1,4-dioxane where 1,2-ethanediol diformate was the main intermediate. However, combination of sonolysis and TiO$_2$ photocatalysis provided a complete degradation of 1,4-dioxane due to an increase of adsorption capacity of the catalyst for 1,2-ethanediol diformate (EDDF). Degradation of 1,4-dioxane was 77% at reaction time 5 min using UV/TiO$_2$ process reaction [45] (Table 2). TiO$_2$ powder was used for degradation of 1,4-dioxane and needs a filtration after mineralization process which should be avoided [128]. Yamazaki et al. [3] successfully used packed bed reactor supplemented with TiO$_2$ pellets for photo degradation of 1,4-dioxane. The removal of 1,4-dioxane was due to adsorption followed by photodegradation process. Photocatalytic oxidation of 1,4-dioxane using the TiO$_2$ sol–gel photo-reactor and UVA light was investigated by Vescovi et al. [15] at pH values of 3 (acidic) and 7 (neutral). 1,4-dioxane was completely removed at both pH values of 3 and 7 at reaction time 60 and 45 min, respectively. However, the P$_{25}$ immobilized system was 5.2 times faster than the TiO$_2$ sol–gel reactor for degradation of 1,4-dioxane due to different characteristics of the titanium dioxide. P$_{25}$ (Degussa) is a highly photoactive commercial catalyst enjoying properties (70% anatase, 30% rutile) to maximize photocatalytic oxidation [46,68,129–131] (Table 2). The main advantage of using TiO$_2$ for photocatalysis process is the ability to reuse the catalyst several times for wastewater treatment [132–134]. However the treatment efficiency using regenerated catalyst is highly fluctuated and depends on the type of contaminants, concentrations and the methods used to recycle the catalyst. Five cycles of the reusability of TiO$_2$ were examined by Alvarez-Corena et al. [45] for 5 min and showed a decrease in the removal efficacy of 1,4-dioxane using TiO$_2$/UV process at increasing the treatment cycles (Table 2). Apparently, the active sites of TiO$_2$ for production of HO$^{\bullet}$ are decreased due to a reduction of UV penetration resulting in deterioration of the efficiency of degradation of 1,4 dioxane.
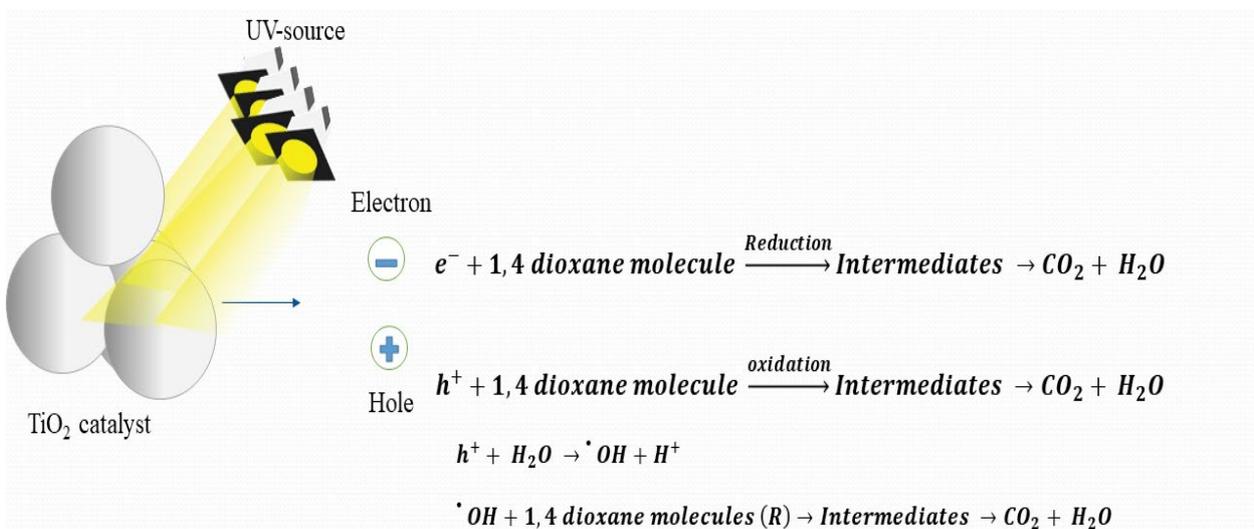

Fig. 5. Titanium oxide (TiO$_2$) for degradation of wastewater containing 1,4-dioxane.

2.2.1.3. Magnetic TiO_2 photocatalyst (MTPC)

Slurry TiO_2 photocatalysis assisted with UVA and solar light was efficient for degradation of 1,4-dioxane and the removal efficiency was much higher than those achieved by the H_2O_2/UVC, UVA or UVC radiation processes [30,46,68,129]. This can be attributed to the large surface area of slurry TiO_2 catalyst which increase the mass transfer between the substrate and the catalyst. However, the drawback of using slurry TiO_2 is recovering of the catalyst which needs solid–liquid separation process. Magnetic photocatalyst (MPC) overcomes such problem where insulated magnetic core particles coated with TiO_2, provides a unique solution to this problem [135]. The application of a magnetic field for separation of the catalyst particles from the treated effluent is possible. However, Coleman et al. [30] found that the removal of 1,4-dioxane was quite low at high loading rate and immobilization of TiO_2 on the reactor walls was more efficient for degradation process (Table 2).

2.2.2. Hybrid photocatalysis processes

2.2.2.1. Immobilized nitrogen and fluorine co-doped titanium dioxide (NF-TiO_2) composite

In fact classical TiO_2-based photocatalysis in slurry suspension requires a subsequent filtration step to reuse the catalyst again which increases the treatment cost. The immobilization of the catalyst in combination with solar light is of great interest to enhance the process engineering where separation and recovery of the catalyst from the process stream is feasible [15,30,136–138]. However, catalyst immobilization could restrict the reactant mass transfer [15,30], which represented the main obstacle of the process. Therefore, immobilized nitrogen and fluorine co-doped titanium dioxide (NF-TiO_2) composite in combination with monodisperse TiO_2 nanoparticles solar photocatalysis was investigated by Barndõk et al. [44] to overcome such phenomena for degradation of 1,4-dioxane. Almost complete removal of 1,4-dioxane ($\leq$100%) was achieved along with 65% of COD and 50% of TOC was removed from industrial wastewater (Table 2). Ethylene glycol diformate, ethylene glycol mono-formate and formic acid were the main reaction intermediates.

2.2.2.2. Photoelectro-peroxone

Combination of individual AOPs (O_3, H_2O_2, UV and electrolysis) will have significant synergistic effects for 1,4-dioxane degradation where a higher HO$^{\bullet}$ radicals are generated [139–144] (Table 3). Combination of ozonation, UV photolysis and electrochemical hydrogen peroxide (H_2O_2) generation is PEP process [145]. Ozone/oxygen (O_2/O_3) gas mixture is passed into a reactor which is supplied with a UV lamp and equipped with carbon-based cathode to convert O_2 into H_2O_2 (Eq. (32)). The in-situ generated H_2O_2 will react with the sparged O_3 or UV to generate $^{\bullet}$OH (Eqs. (33) and (34); Table 3) [146,147]. Furthermore, UV photolysis of O_3 will generate $^{\bullet}$OH radicals (Eq. 35) [147]. Shen et al. [148] showed that the combination of ozonation, ultraviolet (UV) and electro-generation of H_2O_2 provided 33 times of 1,4-dioxane degradation higher than those registered for sole addition

of oxidants. This is mainly due to the presence of multiple ways of $^{\bullet}$OH generation in the PEP process which significantly enhanced and improved the degradation of 1,4-dioxane compared with the single processes (O_3, UV and electrogeneration of H_2O_2) as well as their dual combinations (UV/O_3 and the electro-peroxone [EP] process). The PEP process is a more cost-effective and a safer alternative for removal of 1,4-dioxane as compared with traditional UV/O_3/H_2O_2 process due to production of H_2O_2 is in-situ using O_2. This will not only reduce the cost for purchasing external H_2O_2 reagent but also avoid the risks associated with the storage and handling of this compound.

2.2.2.3. Coagulation-photocatalysis

TiO_2 catalyst is injected into a rapid mixing tank where the coagulants are supplied and subsequent photocatalysis of 1,4-dioxane is occurred in flocculator (slow mixing tank) equipped by UV lamp. The classical coagulation–flocculation process was very poor for removal of 1,4-dioxane [149]. Supplementation of TiO_2 /UV onto a coagulation–flocculation water treatment process completely (100%) removed 1,4-dioxane within 1.0 h [149]. However, the removal efficiency of 1,4-dioxane was substantially dropped (60%) in a continuous flow reactor at contact time and UV dose of 39 min. and 0.35 W/L, respectively. The authors replaced artificial UV by solar UV (0.25 W/L) and found that 100% of 1,4-dioxane was removed within 150 min.

2.2.2.4. Membrane photo-reactor

AOPs usually need further treatment for complete removal of 1,4-dioxane avoiding accumulation of intermediates in the treated effluent. The use of dispersed TiO_2 catalyst is preferable to increase the photocatalytic activity, HO$^{\bullet}$ radicals, mass transfer and reaction rate [150–155]. Stand-alone TiO_2 + UV/MPR combines those advantages where the catalyst could be easily separated and remained in the reaction medium for continuous degradation of 1,4-dioxane [156,157]. The membrane is mainly used for catalyst recovery and producing good effluent quality [152,158]. Photocatalytic membranes provide dual functionalities of photocatalysis and separation process [159–162]. Light radiation onto the membrane surface needs further investigation. Nevertheless, MPRs have several advantages, that is, utilization of suspended catalyst, maximal use of active surface area and control of hydraulic and solids retention times [163–165]. Lee et al. [166] found that the photocatalytic degradation efficiencies of 1,4-dioxane in continuous MPR increased from 74% to 94% at increasing the hydraulic retention time (HRT) from 1.43 to 8.57 h, respectively.

2.2.2.5. Titania (TiO_2– $Cs_{2.5}H_{0.5}PW_{12}O_{40}$) ($Cs_{2.5}$) hybrid films

Combination of solid surface acidity with TiO_2 will certainly improve the photocatalytic performance of organic pollutants where adsorption of contaminants and decomposition of intermediates will be subsequently increased [48]. Moreover, a high quantum yield is expected due to suppression of recombination between electrons and holes on the surface of TiO_2 [68,128,167–169]. Photocatalytic

decomposition of 1,4-dioxane in water was examined by Maurino et al. [68] and Hill et al. [46] and ethylene glycol diformate (EGDF) was the main intermediate. Decomposition rate of EGDF was quite low due to poor affinity with TiO$_2$ [128]. Fortunately, once EGDF is removed and/or oxidized, no intermediate with a slow decomposition rate exists in the reaction medium. Therefore, promotion of EGDF decomposition is necessary for complete mineralization of 1,4-dioxane. Nakajima et al. [48] successfully prepared titania-Cs$_{2.5}$H$_{0.5}$PW$_{12}$O$_{40}$ hybrid films for removal of 1,4-dioxane and EGDF as well. The holes of titania-Cs$_{2.5}$H$_{0.5}$PW$_{12}$O$_{40}$ hybrid films serve as adsorption sites for ethylene glycol diformate and the catalyst was very efficient for photocatalytic decomposition of 1,4-dioxane as compared with sole TiO$_2$ catalyst.

2.2.2.6. Sonolysis and photocatalysis

Ethylene glycol diformate (EGDF) is a main intermediate and the slowest decomposition rate during photocatalysis of 1,4-dioxane using TiO$_2$. Sun et al. [170] found that the desorption capability of sole TiO$_2$ for removal of dibenzofurans was improved by surface modification with fluoric acid solution. US + UV + HF–TiO$_2$ provided higher absorption capability for both 1,4-dioxane and EGDF as compared with pure TiO$_2$ and subsequently enhanced the photocatalysis decomposition rate. These results were confirmed by Suzaki et al. [171], where the Luis acidity of TiO$_2$ surface was increased by hydrofluoric acid treatment. Moreover, sonolysis effectively enhanced the catalyst activity probably due to surface activation, aggregation breakage, or the enhancement of mass transport. Sun et al. [170] and Nakajima et al. [128] found that the enhancement of interaction between the surface acid sites on HF–TiO$_2$ and the π-electrons of the EGDF was occurred on C=O bonding resulting a higher adsorption capability.

3. Factors affecting photocatalytic oxidation processes

The pH value, catalyst concentration (surface area), initial concentration of the contaminants, UV radiant flux, UV wavelength and type of photocatalyst are the major parameters affecting on the photocatalytic degradation process
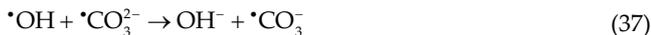
3.1. Effect of pH

The photocatalytic oxidation process is occurred at the outer surface of the catalyst [172] where Sharma et al. [173] found that the degradation rate constants as a function of the pH of the water sample was first order reaction. The highest degradation rate constant of 1,4-dioxane using TiO$_2$/UV was taken place at pH value of 5.0 [45]. However, Coleman et al. [30] reported that 1,4-dioxane degradation on TiO$_2$ photocatalyst was increased under alkaline and acidic conditions. pH value of 3 was suitable for 1,4-dioxane degradation and completely disappeared at pH level of 11. Moreover, complete degradation of intermediate products are also pH dependent, that is, ethylene diamine tetra acetic acid (EDTA) was degraded at pH value of 11 and EGDF resulted from degradation of 1,4-dioxane is taken place at lower pH values [68,174,175]. Photocatalytic degradation of 1,4-dioxane at pH values of 3,7 and 11 using a P$_{25}$ slurry photo-reactor system and UV-A light was investigated by Vescovi et al. [15]. Complete removal of 1,4-dioxane was occurred at all pH

values within 3.0 min. However, the removal of 1,4-dioxane was faster at pH values of 7 and 11. Ethylene glycol diformate was the main intermediate product at pH value of 3 and 7 and was not detected at pH 11. The adsorption capacity, the distribution of hydroxyl radicals and surface charge of titanium dioxide is highly pH dependent [69]. The point of zero charge (pzc) of TiO$_2$ varied from 6.3 to 6.8 [176]. At neutral pH value of 7, the catalyst have no charge and allowing molecules to be easily reach the catalyst surface resulting a high initial reaction rates. On the other hand, complex electrostatic interactions between the molecules and the catalyst in acidic and alkaline conditions would reduce 1,4-dioxane removal. Nevertheless, the surface of the TiO$_2$ is highly hydroxylated at alkali pH [177], which would enhance the reaction rate. Probably, competition for hydroxyl radicals by carbonate ions (CO$_3^{2-}$) is occurred at pH value of 11 where carbon dioxide, mineral acids and water are formed due to complete mineralization of 1,4-dioxane. Carbonic acid would dissociate into the carbonate ion (CO$_3^{2-}$) at pH 11. Carbonate ions are radical scavengers, reacting with hydroxyl radicals to produce the less effective carbonate radical (CO$_3^{\bullet-}$) [178]. The presence of carbonate ions in the reaction medium as a radical scavenger slows down the degradation of 1,4-dioxane [178]. Barndõk et al. [42] showed that 1,4-dioxane was completely removed using ozone (O$_3$) at pH ≥ 9.0 and was quite low (<15%) at pH 7.0 ± 0.1. This indicates that the oxidant O$_3$ was ruled out for the treatment of 1,4-dioxane at neutral pH value [67,176,179] and the decomposition of O$_3$ into HO$^\bullet$ was negligible [52,62,65] which supposed to react with the substrate [176]. This reaction mechanism of HO$^\bullet$ production is initiated by hydroxide anions at high pH values [180,181] and the conversion of O$_3^{\bullet-}$ into HO$^\bullet$ is occurred as reported earlier in the literature [182,183]. Moreover, the authors showed that the 1,4-dioxane degradation reaction was significantly faster using ozone at pH ≥ 9.0 than those the reaction rate at pH of 7.0 ± 0.1. The photocatalytic degradation and mineralization of EGDF using UV/TiO$_2$ was superior at pH 5 compared with pH 3 [184]. Nevertheless, the initial photocatalytic degradation and mineralization rates of EDDF using UV/TiO$_2$/Cu^{2+}, at pH 5 were comparable with pH 3. However the photocatalytic degradation and mineralization at pH 5 were quite slow.

3.2. Effect of carbonate and bicarbonate

Photocatalytic degradation rate of 1,4-dioxane at different alkalinity concentrations was examined by Jung et al. [78] in membrane photoreactor (MPR) treating textile wastewater. 1,4-dioxane degradation rate was sharply declined at increasing the alkalinity level up to 200 mg/L as CaCO$_3$. This can be attributed to consumption of the photocatalytically generated HO$^\bullet$ radicals in the presence of bicarbonates (Eq. (36)). The carbonate and bi-carbonate ions were considered HO$^\bullet$ scavengers [78,185] (Eqs. (36) and (37)). However, Barndõk et al. [43] found that the presence of carbonates (9.0 ≤ pH ≤ 10.0) enhanced the removal of COD (>90%) as compared with neutral conditions due to the carbonate buffer kept the pH level in the optimal range during the ozonation of 1,4-dioxane.

$$^\bullet OH + HCO_3^- \rightarrow H_2O + {^\bullet}CO_3^- \tag{36}$$

$$^{\bullet}OH + {}^{\bullet}CO_3^{2-} \rightarrow OH^- + {}^{\bullet}CO_3^- \qquad (37)$$

3.3. Effect of catalyst surface area

The increase in TiO_2 concentration created a high surface area and more active sites available for the oxidation of 1,4-dioxane. Nevertheless, the ability of the UV radiation to reach the surface of TiO_2 is decreased at high concentrations of the catalyst due to the reduction of the effect of UV light and/or scattered by the catalyst [186]. The effect of different concentrations of TiO_2 on the photocatalytic degradation of 1,4-dioxane was investigated by Alvarez-Corena et al. [45]. The catalyst dosage was varied from 0.1 to 2.5 g/L and the degradation rate of 1,4-dioxane was maximized at TiO_2 concentration of 1.5 g/L. TiO_2-photocatalysis achieved complete mineralization of 1,4-dioxane [15,30]; however, the turbidity is increased at high concentrations of TiO_2 [187,188] resulting a low penetration of light and negatively affected on the quality of treated effluent. Thus, the activation of TiO_2 is necessary. Vescovi et al. [15] found that the P_{25} photo-reactor system in slurry for removal of 1,4-dioxane was superior the immobilized TiO_2 systems due to the higher surface area of the catalyst available in the reaction medium.

3.4. Effect of UV source

Photocatalytic degradation of 1,4-dioxane on TiO_2 was quite similar using either UV-assisted or solar photocatalysis [43]. 45% of 1,4-dioxane was degraded at 360 kJ/L of either solar or UV radiation. Further improvement of 1,4-dioxane removal (60%) occurred at irradiation in solar simulator (470 kJ/L). This indicates that further removal of 1,4-dioxane is possible at long radiation time. The application of solar simulator above the water surface layer is more effective in a large bulk liquid. The light intensity in the turbid catalyst suspension was only 5% at water depth of 1cm. UV-catalyzed process produced much higher intermediates in terms of EGDF and formic acid. Acetic acid was negligible and the mixture of methoxy acetic and glycolic acids were at a level of 5.6 ± 0.2 mg/L [44]. The P_{25} immobilized system was more efficient for removal of 1,4-dioxane as compared with TiO_2 sol–gel photo-reactor due to a high photoactivity of the catalyst in the reaction medium [15]. Photocatalytic degradation of 1,4-dioxane at different UV doses of 0–0.35W/L was investigated by Lee and Choo [149]. They found that no 1,4-dioxane degradation was occurred without UV irradiation and the amount of 1,4-dioxane lost by adsorption onto TiO_2 was negligible. 1,4-dioxane degradation was completed at a reaction time of 50 min and UV dosage of 0.35 WL/L. Moreover, 1,4-dioxane was completely removed (100%) under artificial and solar UV irradiation at a dosage of <1.0 kJ/L. Solar radiation with an average UV dose of 0.12 and 0.27 WL/L was sufficient for 1,4-dioxane degradation [149]. Likely, solar photocatalysis of 1,4-dioxane by MPR was efficient and provided similar results using artificial UV irradiation [149].

3.5. Effect of addition of H_2O_2

Several researchers [189–191] investigated the effect of H_2O_2 addition on photocatalytic degradation of organic pollutants at optimum catalyst loading rate and the degradation process was improved. However, others [192,193] reported a negative impact of adding hydrogen peroxide for degradation of some organic contaminants. The effect of the addition of H_2O_2 on the photocatalytic oxidation of 1,4-dioxane using P_{25} and MPC systems was investigated by Coleman et al. [30]. Addition of 3 ppm H_2O_2 to the P_{25}/UVA slightly increased the degradation rate of 1,4-dioxane. 3 ppm of H_2O_2 was required for photocatalytic degradation of 0.36 ppm 1,4-dioxane using P_{25} based on the molar ratio of H_2O_2/substrate. Therefore, increasing the H_2O_2 will cause a decrease in reaction rate. H_2O_2 would enhance the reaction by providing additional hydroxyl radicals via trapping of photogenerated electrons (Eqs. (38) and (39)) [194] and/or photolysis of H_2O_2 (Eq. (40)).

$$TiO_2\text{-}UV \rightarrow h^+ + e^- \qquad (38)$$

$$H_2O_2 + e^- \rightarrow OH^- + OH^{\bullet} \qquad (39)$$

$$H_2O_2\left(hv, \lambda < 300\text{ nm}\right) \leftrightarrow 2OH^{\bullet} \qquad (40)$$

However, the degradation rate of 1,4-dioxane was slightly decreased with the addition of 5 ppm H_2O_2. This might be due to a slight increase of hydroxyl radicals which will generate less active hydroperoxyl radicals (HOO$^{\bullet}$) (Eq. (41)).

$$H_2O_2 + OH^{\bullet} \rightarrow H_2O + HO_2^{\bullet} \qquad (41)$$

$$HO_2^{\bullet} + OH^{\bullet} \rightarrow H_2O + O_2 \qquad (42)$$

Addition of excessive dosage of 30 ppm H_2O_2 to the P_{25} photocatalytic system substantially reduced the degradation rate 1.7 times due to a combination of formation of less reactive hydroperoxyl radicals (Eq. (41)) and competition of H_2O_2 with the contaminants for conduction band electrons [194]. H_2O_2 consumed hydroxyl radicals (Eqs. (41) and (42)) [195]. Radical–radical recombination occurred (Eq. (42)). Addition of H_2O_2 to the MPC photocatalysis system is quite different where 3 or 5 ppm caused an increase in the degradation rate of 2.5 times for 1,4-dioxane and the addition of 30 ppm H_2O_2 increased the photocatalysis by 3.8 times [30]. This is probably due to the low activity of the MPC compared with P_{25} for generation of hydroxyl radicals. Moreover, addition of H_2O_2 will increase the removal rate with increasing number of hydroxyl radicals present in the reaction medium (Eq. (39)) [196] and suppress recombination of electron–hole pairs produced at the catalyst surface [194]. The role of H_2O_2 in the photocatalytic degradation of 1,4-dioxane is still unclear and needs further research particularly positive or negative effects depending on the irradiation (i.e., wavelength, intensity), pH values, substrate concentration, catalyst type and the molar ratio of oxidant to contaminant [194]. Those parameters are necessary to be considered for H_2O_2/UV/photocatalyst system. This was not the case for Barndõk et al. [42] where the removal of COD and 1,4-dioxane remained unaffected with addition of H_2O_2 to ozonation process at pH ≥ 9.0. This can be attributed to the increase of hydroxide anions resulted from decomposition

of O$_3$ into OH$^\bullet$ radical [180,181]. However, the elimination of 1,4-dioxane was improved with supplementation of H$_2$O$_2$ to ozonation process at pH 7.0 ± 0.1. Apparently, the H$_2$O$_2$ contributes to the generation of OH$^\bullet$ from conversion of O$_3^{\bullet-}$ [182,183] at neutral pH (Eqs. (43) and (44)).

$$HO_2^- + O_3 \rightarrow HO_5^- \tag{43}$$

$$HO_5^- \rightarrow HO_2^\bullet + O_3^{\bullet-} \tag{44}$$

3.6. Effect of ionic strength

1,4-dioxane degradation is quite slow at high ionic strength of the solution and inhibited at ionic strength exceeding 0.2 M/L [91] due to an increase of radical scavenging chloride ions. Likely, chloride ions have been shown to inhibit persulfate oxidation of trichloroethene (TCE) and methyl tert-butyl ether (MTBE) [197,198]. Moreover, increasing initial calcium chloride concentration caused a drop in pH of the solution due to formation of calcium monohydrate phosphate (CaHPO$_4$), resulting in a decrease of buffering capacity. Cloudy precipitate was observed in the higher CaCl$_2$ concentration solutions (7 and 70 mM/L) [91].

3.7. Effect of applying voltage

Photocatalytic decomposition of 1,4-dioxane initially produced ethylene glycol diformate (EGDF) [46,68] which represented the slowest degradable intermediate products resulted from the reaction. Accumulation of EGDF in the reaction medium causes a severe problem for degradation of 1,4-dioxane. Therefore, degradation of EGDF represented the most step for complete removal of 1,4-dioxane using photocatalyst. Moreover, the removal of EGDF will facilitate and enhance the subsequent reaction processes. Combination of sonolysis and photocatalysis accelerate the degradation of EGDF [128]. Yanagida et al. [199] found that photocatalytic degradation rate of 1,4-dioxane depends on applying voltage where ethylene glycol diformate (EGDF) and 1,4-dioxane exhibited inverse voltage dependence. Applying voltage enhanced photocatalysis of 1,4-dioxane and surprisingly suppressed EGDF formation [199,200].

3.8. Effect of catalyst loadings

1 g/L TiO$_2$ loading is the optimum catalyst loading for the removal of 1,4-dioxane using P$_{25}$ photocatalyst [30]. However, the removal rate of 1,4-dioxane was slightly increased from 2.2 and 2.4 μgC/min at increasing the catalyst loading from 0.1 to 1 g/L respectively. 1 g/L of P$_{25}$ TiO$_2$ was the optimum loading for the degradation of organic substances in contaminated water [30,201]. Mehrvar et al. [129] found that 1.5 g/L was the optimum loading for removal of high concentration of 1,4-dioxane (27.8 ppm). This was not the case for MTPC where 0.1 g/L was the optimum and provided similar removal efficiency of 1,4-dioxane using 1 g/L of P$_{25}$ TiO$_2$. The removal rate of 1,4-dioxane was dropped from 0.24 to 0.18 μgC/min at increasing the MTPC catalyst loading from 0.1 to 1.0 g/L, respectively. This was attributed to the particle size and the light scattering characteristics of the photocatalysts [30].

5 g/L TiO$_2$ catalyst was required to maximize 1,4-dioxane degradation in MPR. Lee et al. [166] found that the 1,4-dioxane degradation rate was increased at increasing TiO$_2$ dosage from 0.1 to 1.0 g/L. 100% of 1,4-dioxane was removed at contact time and TiO$_2$ dosage of 50 min and 1.0 g/L, respectively. Moreover, photocatalytic intermediates were not detected in the reaction medium.

3.9. Effect of turbidity

Water turbidity would affect photocatalytic reactions due to light scattering [202,203]. The effect of feed-water turbidity on the degradation of 1,4-dioxane was examined by Lee and Choo [149] for a range of 0.1 to 115 NTU. The authors concluded that there is no effect of the turbidity on the degradation efficiency of 1,4-dioxane in this range.

3.10. Effect of dissolved oxygen (DO)

DO as an electron acceptor in the photocatalytic reaction medium particularly using TiO$_2$ would play a necessary role to avoid the recombination of photo-generated charge carriers. The photocatalytic degradation of 2,3-dichlorophenol was improved in the presence of DO [204] dichloroacetic acid [205], 2-chlorobiphenyl [206], etc. Oxygen reacts only slowly with the electrons and the electron transfer rate from TiO$_2$ to oxygen can control photocatalysis process [207]. Youn et al. [208] found that the photodegradation of 1,4-dioxane by TiO$_2$ was substantially increased at increasing the DO levels in the reaction medium and the 1,4-dioxane was almost completely degraded at contact time of 8 h under high DO conditions. Similar results were observed for photodegradations of organic contaminants by TiO$_2$ [204–209]. This promoting effect of the DO on photodegradation of 1,4-dioxane is mainly due to the role of DO as an electron scavenger which certainly assists to reduce electron–hole recombination.

3.11. Effect of nanoparticles addition

The recombination of photogenerated electron–hole pairs needs to be suppressed to enhance the photocatalytic activity of TiO$_2$. Noble metals, that is, Au (1.2 wt.%) nanoparticles were incorporated with TiO$_2$ to efficiently separate charge carriers created in/on catalyst [208] promoting the photocatalytic activity of the catalyst. Nano-sized Pt and Ag particles loaded on TiO$_2$ were applied for photodegradation of oxalic acid and the photocatalytic activity was increased as compared with only TiO$_2$ [210]. Photocatalytic degradation of lignin was increased six times in the presence of combination of Pt/TiO$_2$ [211]. The Au-capped TiO$_2$ nanoparticles increased the photocatalytic efficiency of thiocyanate by a value of 40% [212]. TiO$_2$ modified with nano-sized Au provided a higher activity for the mineralization of oxalic acid than those observed for a commercially available TiO$_2$ [213]. Au nanoparticles incorporated with TiO$_2$ enhanced the photocatalysis process at low loading of nanoparticles. This was not the case for high loading of the catalyst (0.35% Au) [24,25] due to the inhibition of adsorption of 1,4-dioxane or hydroxyl species on TiO$_2$ surface.

3.12. Effect of copper (II) ions

Heterogeneous photocatalysis using TiO_2 represents the most attractive process for degradation of 1,4-dioxane where it is effective for a wide range of pH values. Nevertheless, the most drawback of the process is that the photogenerated electron–hole pairs can recombine resulting in low quantum efficiency [214,215]. Transition metal ions, that is, Cu^{2+}, Fe^{3+} or Mn^{2+} have the capability to trap the photogenerated electron (Eq. (45)) [216–221] and subsequently improve the efficiency of TiO_2 catalyst.

$$M^{n+} + e^-_{cb} \rightarrow M^{(n-1)+} \tag{45}$$

Lam et al. [222] found that the addition of Cu^{2+} enhanced the photocatalytic degradation and mineralization of 1,4-dioxane at pH values ranging from 3 to 5. This was due to the involvement of Cu^{2+} in the ligand-to-metal charge transfer process, where Cu^{2+} formed complexes with 1,4-dioxane and/ or intermediate products resulting in an alternative oxidation reaction route. Moreover, Cu^{2+} increased the oxidation of EGDF at pH 3 resulting in a complete mineralization of 1,4-dioxane. Cu remained in dissolved state at pH 3 and the total dissolved Cu concentration dropped at pH 5 resulting

in retardation in the photocatalytic oxidation of EGDF due to the formation of insoluble Cu species. The presence of the insoluble Cu species negatively affects light penetration and subsequently reduces the availability of dissolved Cu^{2+} to interact with the intermediate product of EGDF in the reaction medium.

4. Fate of 1,4-dioxane and intermediate by-products

AOPs were used for the removal of 1,4-dioxane from water/wastewater. However, several intermediates, that is, aldehydes, organic acids, mono- and diformate esters of 1,2-ethanediol are generated due to the oxidation of the 1,4-dioxane. The formation and degradation of intermediates are mainly affected by catalyst type, dosage, pH values, illumination (irradiation) time, etc. •OH radicals attack 1,4-dioxane molecules resulting in H⁻ abstraction to form 1,4-dioxanyl radical which is further oxidized by available dissolved oxygen to form peroxyl radical (Fig. 6) [223]. The latter undergoes bimolecular decay to form tetroxide intermediates [223,224]. Two oxyl radicals and O_2 are formed due to the decomposition of tetroxide. The termination reactions of peroxyl radical generate the tetroxide precursor of 1,4-dioxan a-oxyl radical, which is finally produced
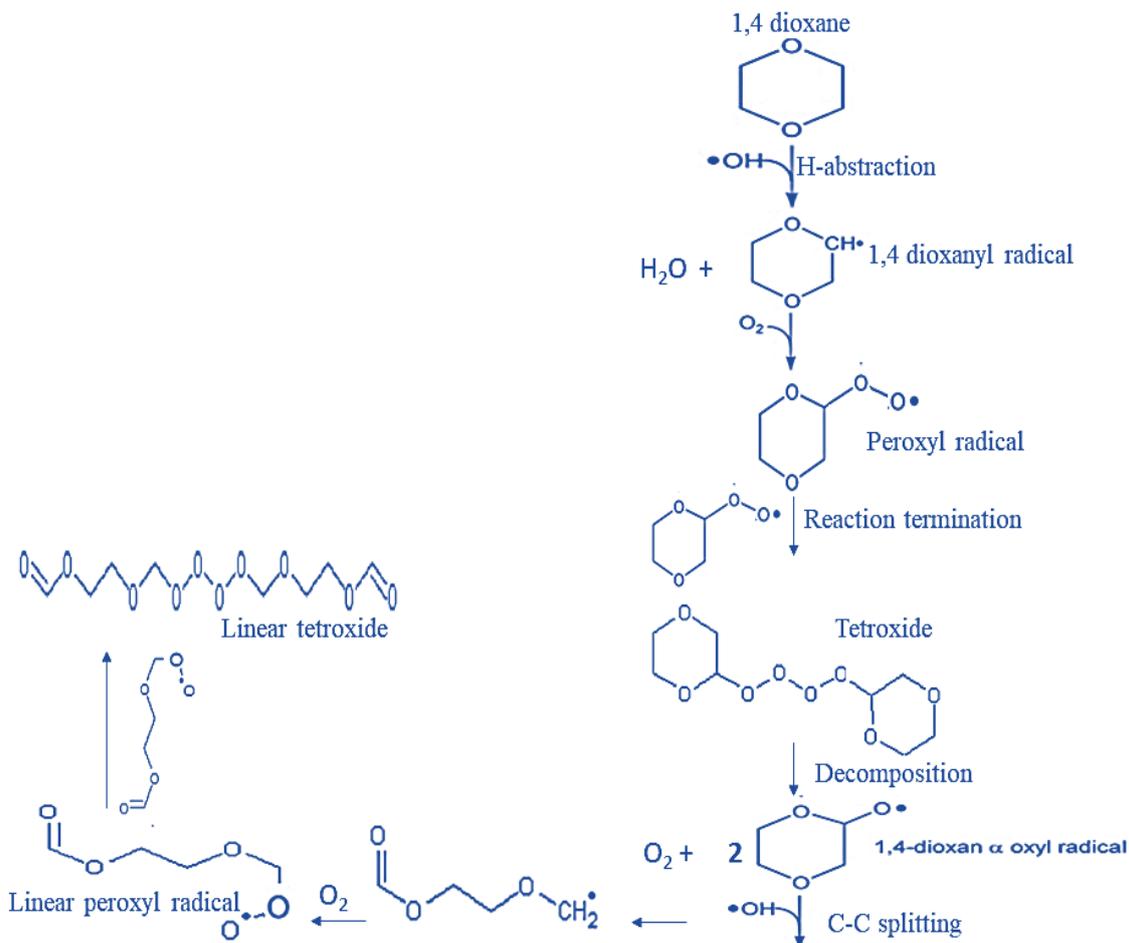

Fig. 6. Main reaction mechanism of homogenous, heterogeneous and catalytic oxidation of 1,4-dioxane.

releasing oxygen [13,37,98]. 1,4-dioxan a-oxyl radical ring is opened due to splitting of the ΔC–C bond resulting in linear peroxyl radical which reacts with oxygen to produce a linear tetroxide [223–225]. Two further reactions for linear tetroxide occurred, that is, (1) the electro-cyclic process where ethylene glycol diformate (EGDF) is produced [13,37], or (2) the decomposition into two alkoxyl radicals and oxygen followed by Regular-fragmentation and H abstraction to form ethylene glycol monoformate (EGMF) and formic acid [13,36,43,226] (Fig. 7). Likely, Barndõk et al. [42] found that EGDF was the major primary intermediate in TiO_2-photocatalysis and photo-Fenton process. However, in heterogenous photo-Fenton process using Fe^0, scheme 3 was proposed by Barndõk et al. [42,43] where an alternative degradation mechanism of 1,4-dioxane via methoxyacetic and acetic acid occurred. Beckett and Hua [37] found that glycolic acid and formic acid resulted from the degradation of methoxyacetic acid. Finally, ethylene glycol and formic acid are formed due to acid hydrolysis of mono- and diformate ethylene glycol [227] (Fig. 7). Ethylene glycol may be degraded into glycolic acid followed by oxalic acid by deformulation [228]. Oxalic acid appeared as oxalate anion under acidic pH values resulting in the reaction pathway in Fig. 8. 1,4-dioxan-a-oxyl radical is the main primary intermediates of the degradation of 1,4-dioxane and generated due to formation of tetroxide (Fig. 6) [13,36,226]. The a-oxyl radical is degraded either through ΔC–C splitting at the a-C position (Fig. 8) or via an intramolecular reaction (H abstraction from the a-C position) followed by fragmentation (Fig. 8) [13]. 1,4-dioxan-a-oxyl radical is degraded through an intramolecular reaction to produce formaldehyde and formic acid along with the carbon-centered radical (Fig. 8).

The formed radicals are reduced into methoxy-acetaldehyde and subsequently oxidized to methoxy acetic and acetic acid. β-scission yielding acetaldehyde and consequently, acetic acid is another alternative intermediates [10,35,36]. Barndõk et al. [43] found that acetic acid was detected using $Fe^0/H_2O_2/$UV. The conversion of acetic acid yields free-radical-induced degradation by-products such as formaldehyde, glycolic and glyoxylic acids. CO_2 is produced in that stage of decomposition indicating that some mineralization occurred [223,228,229]. The EGDF was the main intermediate by product and the formation of methoxyacetic acid was minor for ozone oxidation of 1,4-dioxane at acidic conditions [57]. Stefan and Bolton [13] found that 90% of the initial concentration of 1,4-dioxane was depleted using $O_3/H_2O_2/$UV at the 1st 5 min of irradiation and 1,2-ethanediol mono and diformate esters, formic acid and methoxyacetic acid were detected in the treated effluent. The decay of EGDF is pH and reaction type dependent which is rapidly hydrolyzed into ethylene glycol (Fig. 9) [8] using Fe^0-based photo-Fenton at pH_0 of 8.5 and classical Fenton process at acidic condition (pH_0 2.8) [36]. Similar pathway of acid-catalyzed hydrolysis was occurred in the $Fe^{2+}/H_2O_2/$UV process [43]. Ethylene glycol is subsequently degraded and hydrolyzed into glycolic acid through formation of glycol aldehyde [36] and some of formic acid was detected as well. The hydrolysis of EGDF into ethylene glycol was negligible at pH_0 value of 5.7 in UV/TiO_2 process [43]. At a high reaction rate with ·OH, formic acid was mineralized into CO_2 [13,223,230]. Glycolic acid decomposes into glyoxylic acid which is further oxidized to oxalic acid [36,223,228]. Oxalic acid is the last intermediate for mineralization of organics [42,13,223]. Glyoxylic acid decomposes into oxalic acid, which is easily converted
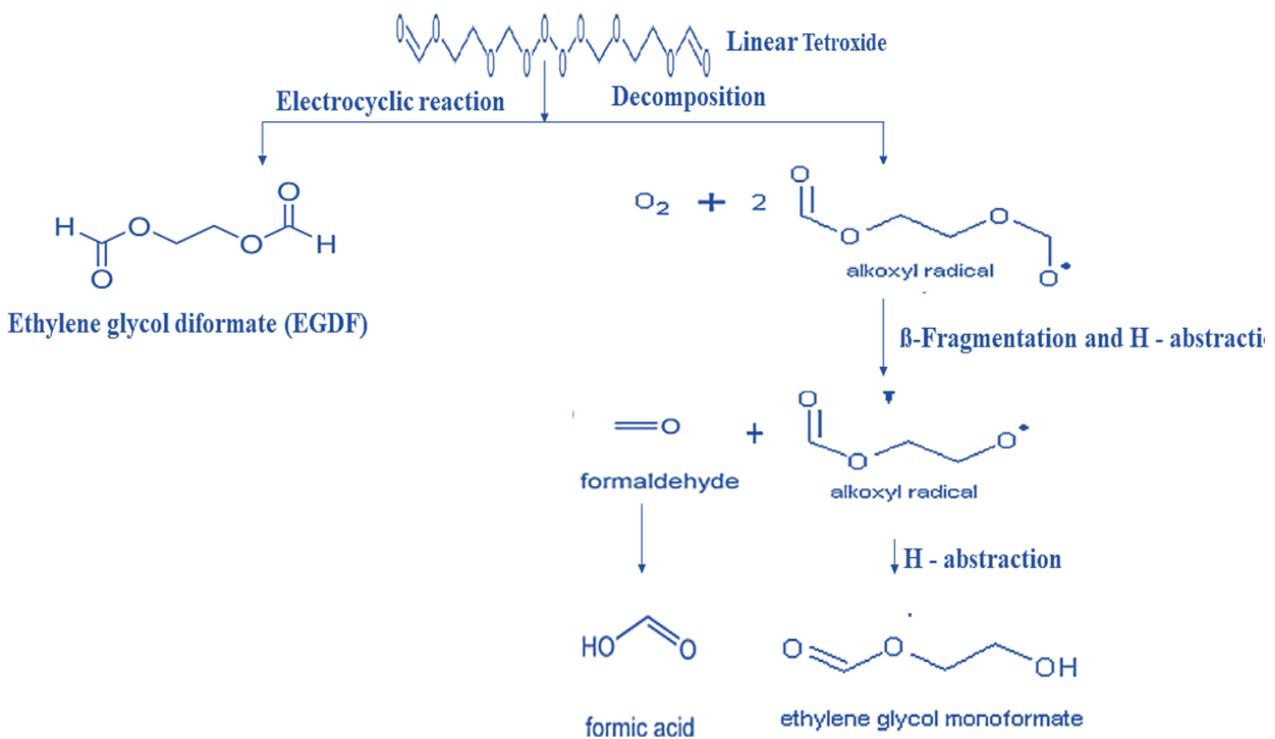

Fig. 7. Degradation of linear tetroxide into ethylene glycol diformate (EGDF) and monoformate (EGMF).
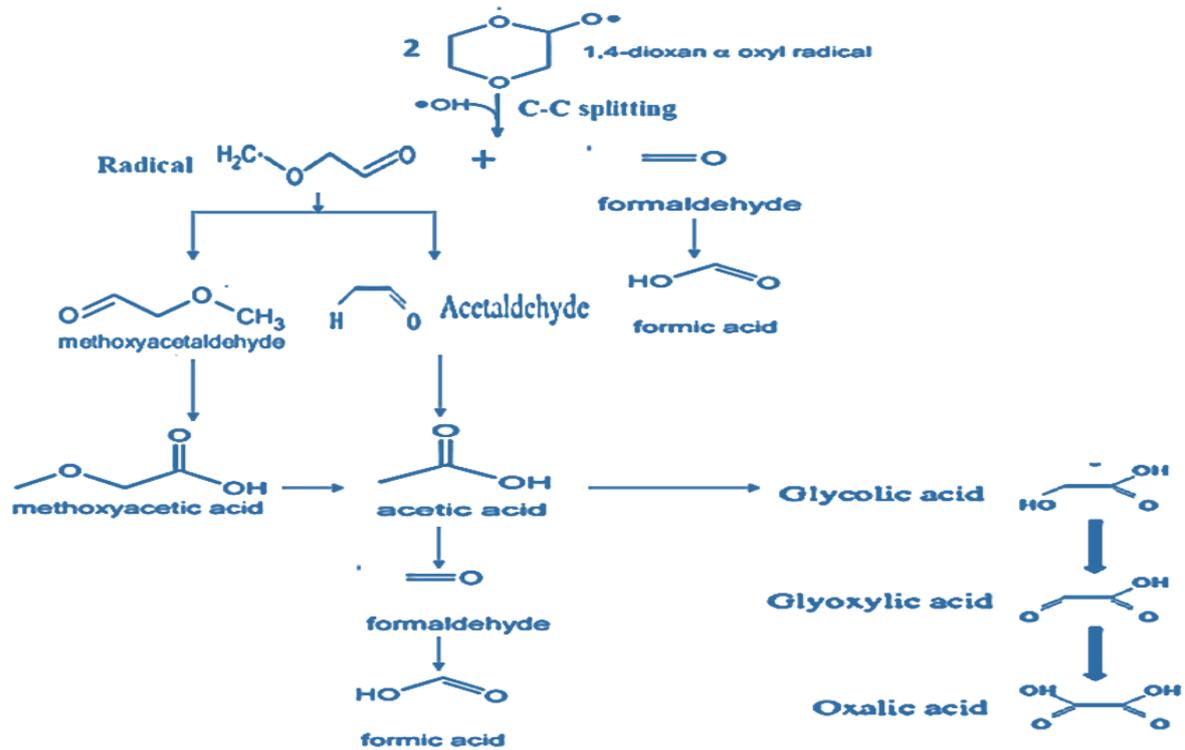
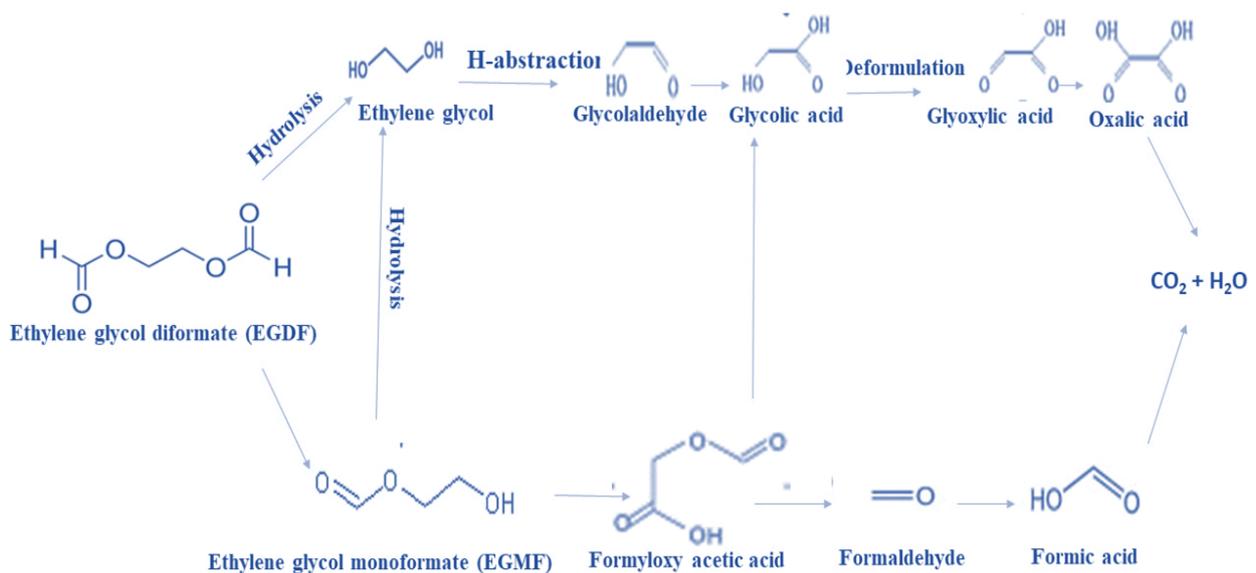Fig. 8. Fate of 1,4-dioxane a-oxyl radical during oxidation of 1,4-dioxane.

Fig. 9. Degradation of ethylene glycol diformate (EGDF) and monoformate (EGMF).

into water and CO_2 [223,228]. Lam et al. [231] found that the photocatalytic oxidation of 1,4-dioxane at pH 3 occurred in a two-step reaction controlled by the degradation of EGDF and at pH value of 5, more complex processes were observed. Residual values of EGDF were detected at pH of 3 and 7. However, the degradation of EGDF was slightly faster at pH 7 than at pH value of 3. The EGDF was completely

removed at pH value of 11 [15]. Maurino et al. [68] reported that EGDF was not detected at pH value of 11 and was quickly hydrolyzed into ethylene glycol and formate (>95% in 90 s). Small quantities of ethylene glycol, and relatively high amounts of formaldehyde, glycolaldehyde, formic and glycolic acids were detected at pH 5.5. Mehrvar et al. [174] identified EGDF, formaldehyde and formic, glycolic and

oxalic acids as intermediates during the photocatalytic oxidation of 1,4-dioxane at pH 4. Complete mineralization of 1,4-dioxane in aqueous solution was achieved using light ($A > 300$ nm) and TiO_2. The degradation of 1,4-dioxane using ozonation process at pH > 9 occurred faster via the formation of ethylene glycol. This was not the case for the decomposition of 1,4-dioxane under acidic conditions (pH < 5.7) where the formation of ethylene glycol diformate was occurred and its degradation was quite slow [43].

5. Biodegradation processes

Conventional physicochemical treatment processes such as coagulation and adsorption are not efficient for removal of 1,4-dioxane from industrial wastewater due to its high solubility. AOPs are effective methods for degradation of 1,4-dioxane [13,232]. However, AOP consumes considerably high quantities of chemicals and energy which should be avoided to reduce the operating costs particularly for low income countries. Moreover, 1,4-dioxane was considered non-biodegradable by microorganisms, although some recent investigations have shown its biodegradation under specific conditions. Therefore, biological degradation processes of 1,4-dioxane are very limited in the literature. The indigenous microorganisms were not typically accounted for degradation of 1,4-dioxane [233,234]. However, biodegradation of 1,4-dioxane was taken place in pure [21–23] and mixed cultures bacteria [24]. Furthermore, Mahendra and Alvarez-Cohen [235] reported that the biodegradation of 1,4-dioxane by different bacteria strongly depends on the community structure and the presence of an extra carbon source. Pure cultures bacteria (*Mycobacterium* sp. and *Pseudonocardia* sp. [22,235,236] and a fungal strain [237] was used for biodegradation of 1,4-dioxane. Likely, monooxygenase-expressing strains were also efficient for removal of 1,4-dioxane [238,239]. Nevertheless, incomplete degradation of 1,4-dioxane was mainly due to insufficient enzymes [240]. A pure culture of *Mycobacterium vaccae* JOB5 was shown to partially degrade 1,4-dioxane, but the bacterial growth was quite limited [22]. The biodegradation of 1,4-dioxane using *Rhodococcus* strain [23] and bacterium (strain CB1190) [21] was quite satisfactory for mineralization of 1,4-dioxane. Recently Vainberg et al. [25] identified three new pure bacterial cultures, that is, strain ENV425 has the capability to degrade 1,4-dioxane after growth on either THF or propane, and it was efficient for degradation of the non-symmetrical alkyl ether methyl-tert-butyl ether [13]. Strains ENV478 and ENV473 efficiently degraded 1,4-dioxane after growth on THF. However, strain ENV478 had the unique ability for degradation of 1,4-dioxane after growth on sucrose, and isopropanol. The growth of ENV478 on THF was enhanced in the presence of 1,4-dioxane, suggesting that the strain obtains metabolic carbon and energy source from 1,4-dioxane. Mixed cultures bacteria were able to degrade 1,4-dioxane, but only in the presence of the co-substrate, that is, tetrahydrofuran (THF) [24]. Currently, there have been very few investigations on the biodegradation of 1,4-dioxane (Table 4). Aerobic biodegradation of 1,4-dioxane was facilitated with mixed cultures, amended with industrially oriented activated sludge [22]. The biodegradability of 1,4-dioxane in the obligate presence of tetrahydrofuran (THF) was investigated using a continuous-flow attached-growth reactor packed with ceramic saddles [236]. Han et al. [241] found that up-flow biological aerated filter is efficient for removal of 1,4-dioxane at low initial concentrations.

5.1. Factors affecting biodegradation process

5.1.1. Effect of pH value

Isolated bacteria had the capability to degrade 1,4-dioxane at pH values ranging from 3 to 10 [242]. However, the acidic pH values could suppress the degradation efficiency of specific strains. The specific 1,4-dioxane degradation rate at pH value of 5.0 was nearly half of those achieved at pH level of 7.5 using strain D17 [243]. The highest degradation efficiencies were registered at pH value of 6–8 [243–245]. Strain N23 was superior to previously isolated bacteria under acidic conditions and provided >80% removal of 1,4-dioxane at pH value of 3.8 [242]. Surprisingly, efficiency of strain N23 was not largely reduced under acidic condition where 30% of the 1,4-dioxane was removed at pH value of 3.1.

5.1.2. Effect of temperature

The effects of temperature on the removal efficiency of 1,4-dioxane using strain N23 were assessed by Yamamoto et al. [242]. The highest 1,4-dioxane-degrading ability of 13.5 mg-1,4-dioxane/L.h was taken place at a temperature of 25°C–35°C, and was kept at a level of 76% at a temperature of 20°C. The degradation efficiency of 1,4-dioxane was fully stopped at temperature exceeding 40°C using strain N23. Likely, Isaka et al. [246] found that the efficiency of polyethylene glycol gel carriers entrapping *Afipia* sp. D1 was adversely affected at different temperatures. 1,4-dioxane removal efficiency increased at increasing the temperature from 6.9°C to 31.7°C. The removal efficiency was highly deteriorated at a temperature exceeding 31.7°C and was 26% at low temperature of 6.9°C.

5.1.3. Effect of substrate concentration

The ability of strain N23 was efficient to utilize various substrates for their growth, that is, 1,4-dioxane, acetic acid, 1,4-butanediol, 1-butanol and glucose), as well as intermediates of 1,4-dioxane degradation (ethylene glycol, glycolic acid and glyoxylic acid [247], 1,4-dioxane analogue (tetrahydrofuran), and diethylene glycol. The growth of strain N23 was optimized in the presence of 1,4-butandiol. Glyoxal (a 1,4-dioxane degradation intermediate [247]), phenol and tri-ethylene glycol (a trimer of ethylene glycol) were not utilized for growth using strain N23. The growth of strain DT8 was inhibited at 1,4-dioxane concentration of >300 mg/L [248]. This is not the case for strain N23 where it was capable of degrading 1,4-dioxane at influent concentration of 1,000 mg/L [246].

5.1.4. Effect of co-substrate addition

The presence of other carbon sources in the reaction medium could enhance 1,4-dioxane degradation. *Mycobacterium vaccae* JOB5 and *Rhodococcus ruber* ENV425 degraded 1,4-dioxane in the presence of alkane [249]. The bacteria

Table 4
Biological processes used for the treatment of wastewater containing 1,4-dioxane

Technology	Operating conditions	Reactor efficiency	References
Activated sludge (electrolytic respirometry process)	Adaptation period of 32 d	150 mg/L of 1,4-dioxane was biodegraded to below detection limit	[253]
Activated sludge	Incubation period of 14 d (co-metabolic degradation with 100 mg/L of tetrahydrofuran (THF)	69% removal efficiency at initial concentration of 1,4-dioxane (100 mg/L)	
Attached and attached-growth reactor packed with ceramic saddles	–	–	[19,236]
Up-flow anaerobic separation gases reactor	–	1,4-dioxane < 1 mg/L at low initial concentrations	[8]
Auto-aerated down-flow hanging luffa (ADHL) system	–	1,4-dioxane < 1 mg/L at low initial concentrations	[1]
Rotating biological contractor	–	Efficient at relatively low 1,4-dioxane concentrations of 1–30 mg/L	[24]
Trickling filter	Module was operated for over 1 year	95%–98% (initial substrate concentration of 0.2–25 mg 1,4-dioxane/L)	[20,35]
Up-flow biological aerated filter		Efficient for removal of 1,4-dioxane at low initial concentrations	[241]
Polyethylene glycol gel carriers entrapping *Afipia* sp. D1	–	Removal efficiency of 1,4-dioxane was highly deteriorated at a temperature exceeding 31.7°C and was 26% at low temperature of 6.9°C	[246]
	–	The residual values of 1,4-dioxane in the treated effluent was 3.6 mg/L at influent concentration of 400 mg/L resulting removal efficiency of 99%	

utilize the alkane as energy source for enzymes production. The alkane oxidation enzymes (monooxygenase) are produced and mainly used for degradation of 1,4-dioxane [250]. Biodegradation of 1,4-dioxane using bacterial strains under co-metabolic conditions was earlier studied [251,252] and the performance was satisfactory accepted. Nevertheless, it is difficult to cultivate those bacteria in wastewater treatment systems without metabolic substrates, that is, tetrahydrofuran or toluene. Supplementation of considerable amounts of chemicals is required as a metabolic substrate for bacterial growth. Furthermore, the metabolic substrate should be removed from the wastewater to decrease the chemical oxygen demand. This is not the case for *Afipia* sp. D1 where no additional chemicals are required for removal of 1,4-dioxane. Moreover, the concentration of intermediates in the treated effluent is quite low using *Afipia* sp. D1 wastewater [246]. *Afipia* sp. D1 produces a relatively higher biomass yield than those reported for *Pseudonocardia dioxanivorans* CB1190 [251]. The estimated u_{max} of 1.8/d was observed for *Afipia* sp. D1 which gave an indication for high growth rate and biomass yield to enhance the start up period. Vainberg et al. [252] found that the biodegradation of 1,4-dioxane using *Pseudonocardia* sp. strain ENV478 resulted in an accumulation of 2-hydroxyethoxy acetic acid in the treated effluent. The efficiency of *Afipia* sp. D1 for removal of 1,4-dioxane was stable and efficient in the presence of the other organic and inorganic pollutants in the wastewater [246]. These results are confirmed by Sei et al. [253] where 1,4-dioxane degradation using strain D1 was not deteriorated in the presence of easily biodegradable compounds such as ethylene glycol at a level of 3,000 mg/L. Isaka et al. [246] found that no significant adverse effect on 1,4-dioxane removal performance by strain D1 entrapped in gel carrier at relatively low nutrients, (20 mg NH_4–N/L and 5.0 mg PO_4–P/L). Presumably, 1,4-dioxane removal performance by strain D1 would not be affected in the presence of other organic substrates and low concentration of nutrients. Monooxygenase enzyme plays a key role for 1,4-dioxane degradation using bacterial strains where hydroxylation of the 1,4-dioxane ring is occurred [251,252,254]. Several species of monooxygenase-producing bacteria, for example, *Pseudomonas putida* mt-2, *Methylosinus trichosporium* OB3b, *Mycobacterium vaccae* LOB5 and *Pseudomonas mendocina* KR, are known to co-metabolically degrade 1,4-dioxane in the presence of methane, propane, THF or toluene. Interestingly, the microbes sequenced into six groups are known to produce soluble methane monooxygenase [252]. Moreover, strains Betaproteobacterium G5G6, *Azoarcus* sp. EbN1 and *Propionivibrio limicola*, categorized into group 5, can degrade toluene. However, these specified microbes still need to be investigated to see if they are able to directly degrade 1,4-dioxane under different experimental conditions. Sei et al. [253] found that the concentration

of 1,4-dioxane (100 mg/L) was reduced by a value of 69% using activated sludge within 14 d via co-metabolic degradation with 100 mg/L of tetrahydrofuran (THF).

5.1.5. Effect of immobilization of pure culture bacteria on the carriers entrapping

Afipia sp. D1 is efficient and has the capability of using 1,4-dioxane as a sole energy and carbon source. Sei et al. [253] found that *Afipia* sp. D1 is very effective for 1,4-dioxane biodegradation as compared with previously reported strains. Isaka et al. [246] successfully applied gel entrapment technology to immobilize aerobic, anoxic and anaerobic bacteria for wastewater treatment. The most advantage of gel carrier is easily moved and separated from wastewater using a screen. The immobilized bacteria cannot be washed out from the reactor creating long biomass retention times for strain D1 to degrade 1,4-dioxane at short HRT. Strain D1 was entrapped/immobilized in a polyethylene glycol gel carrier for removal of 1,4-dioxane from wastewater [246]. The residual values of 1,4-dioxane in the treated effluent was 3.6 mg/L at influent concentration of 400 mg/L resulting in a removal efficiency of 99%. The maximum removal rate of 1,4-dioxane was 0.67 kg dioxane/m³.d at an HRT of 16 h. This was mainly due to an increase in the initial cell concentration in the gel carrier from 6.1×10^5 CFU/mL-carrier to 8.8×10^9 CFU/mL carrier.

5.2. Biodegradation pathway

The microbial degradation of 1,4-dioxane under co-metabolic conditions was common where other organic substrates provided a carbon and energy source for bacterial growth [22,25,255–258]. Recently, some microorganisms have been identified to utilize 1,4-dioxane as a sole source of carbon and energy [21,23,255,256]. Earlier investigations of biological 1,4-dioxane transformation were initially performed as part of toxicological studies where hydroxyethoxyacetic acid (HEAA) and 1,4-dioxane-2-one was the major metabolites by-products in humans [259] and rats [260], respectively. The pathways of 1,4-dioxane biotransformation were investigated using metabolizing and cometabolizing bacteria and fungi to understand the fate of the compound in the environment. The hydroxylation of the 1,4-dioxane ring by monooxygenase enzymes is the first step in the biodegradation process [25,255,257] based on toxicological studies (Fig. 10). The hydroxylated metabolite undergoes uncharacterized biotic or abiotic processing resulting in the opening of the ring structure. Two metabolites, 1,4-dioxane-2-ol and ethylene glycol, were detected using GC-MS analysis in *Mycobacterium* sp. strain PH-06, which was grown on dioxane and deuterated dioxane [261]. 2-Hydroxyethoxyacetic acid (2HEAA) was detected for degradation of ^{14}C-labeled dioxane using cometabolizing bacterium *Pseudonocardia strain* ENV478 [24]. Likely, 1,4-dioxane metabolites was performed using *Pseudonocardia dioxanivorans* strain CB1190 (24) and 2-hydroxyethoxyacetaldehyde, 1,2-dihydroxyethoxyacetic acid, 2-hydroxyethoxy-2-hydroxyacetic acid, glycoaldehyde, glyoxylic acid, and CO_2 were detected and identified by Mahendra et al. [262]. Oxalic acid was identified as the core of central metabolism [262]. *Mycobacterium* sp. PH-06 was isolated by Kim et al. [263] from contaminated river sediment to metabolize 1,4-dioxane resulting in 1,4-dioxane-2-ol and ethylene glycol as major metabolite by-products.
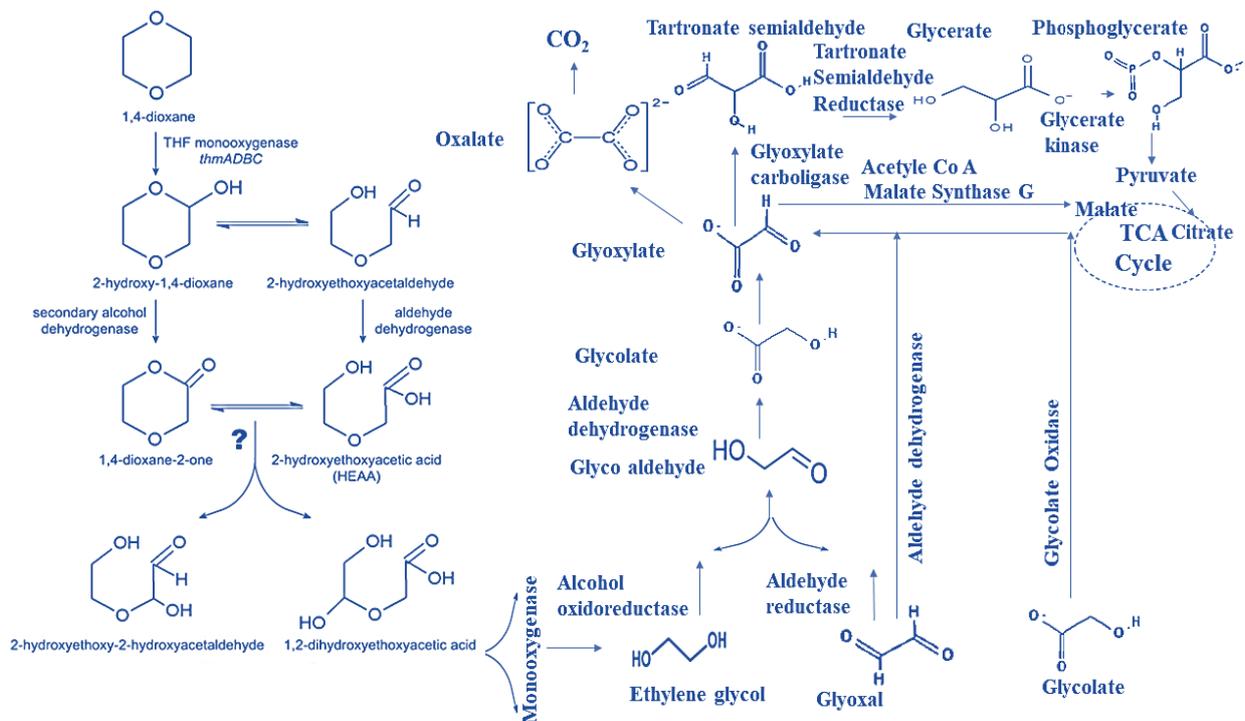

Fig. 10. Biodegradation pathways and enzymes involved in 1,4-dioxane metabolism (adapted from Mahendra et al. [26] and Grostern et al.,[247]).

Pseudonocardia carboxydivorans RM-31 and *Xanthobacter flavus* DT8 were utilized to degrade 1,4-dioxane where the authors found that monooxygenase enzyme was not the initiation enzyme in *X. flavus* DT8 suggesting a different 1,4-dioxane biodegradation mechanism [264]. The bacterial strain of *Pseudonocardia benzenivorans* B5 was able to grow on 1,4-dioxane [265]. *Cordyceps sinensis* fungal strain was reported by Nakamiya et al. [266] to metabolize 1,4-dioxane and produce ethylene glycol, glycolic acid and oxalic acid. Biodegradation of 1,4-dioxane at concentration of 80 mg/L was investigated by Gedalanga et al. [267] where microbial community in activated sludge was able to grow on 1,4-dioxane, that is, CB1190-like bacteria.

6. Future outlook

- Although AOPs are efficient for removal of 1,4-dioxane, potential limitations of the process need to be carefully addressed before implementing the technology at full scale, that is, aldehydes and organic acids formations. Moreover, free hydroxyl radical scavengers (carbonate and bicarbonate) would inhibit contaminant destruction efficiency, which should be addressed.
- Little or no research has been conducted to evaluate 1,4-dioxane degradation under redox conditions (iron reducing, sulfate reducing and methanogenic), which are common in aquifers.
- Studying the effect of co-substrate additives, that is, volatile fatty acids on the degradation of high concentration of 1,4-dioxane using anaerobes.
- Phytoremediation of wastewater containing high concentrations of 1,4-dioxane is a relatively new approach.

Acknowledgment

References

[1] T.K.G. Mohr, Environmental Investigation and Remediation: 1,4-Dioxane and Other Solvent Stabilizers, CRC Press, Boca Raton, 2010.

[2] M. Mahmoud, S. Ismail, A. Tawfik, Post-treatment of anaerobic effluent containing 1,4-dioxane and heavy metals via auto-aerated down-flow hanging luffa (ADHL) system, Process Saf. Environ. Prot., 17 (2018) 22–32.

[3] S. Yamazaki, N. Yamabe, S. Nagano, A. Fukuda, Adsorption and photocatalytic degradation of 1,4-dioxane on TiO_2, J. Photochem. Photobiol., A, 185 (2007) 150–155.

[4] R.E. Jackson, V. Dwarakanath, Chlorinated degreasing solvents: physicalchemical properties affecting aquifer contamination and remediation, Groundwater Monit. Rem., 19 (1999) 102–110.

[5] M.W. Priddle, R.E. Jackson, Laboratory column measurement of VOC retardation factors and comparison with field values, Groundwater, 29 (1991) 260–266.

[6] Environmental Protection Agency, U.S. (US-EPA), Toxicological review of 1,4- dioxane (CAS No. 123–91–1), EPA/635/R-09/005-F, USEPA, Washington, DC, 2010.

[7] Environmental Protection Agency, U.S. (US-EPA), Treatment Technologies for 1,4- Dioxane: Fundamentals and Field Applications, EPA-542-R-06–009, USEPA, Office of Solid Waste and Emergency Response, Washington, D.C., 2006.

[8] M. Mahmoud, A. Elreedy, P. Pascal, Le R. Sophie, A. Tawfik, Hythane (H_2 and CH_4) production from unsaturated polyester resin wastewater contaminated by 1,4-dioxane and heavy metals via up-flow anaerobic self-separation gases reactor, Energy Convers. Manage., 152 (2017) 342–353.

[9] T.K.G. Mohr, Solvent stabilizers white paper. [Online.] Santa Clara Valley Water District, San Jose, California, 2001. Available at: http://www.valleywater.org/Water/Water_Quality/Protecting_your_water/_Solvents/_PD Fs/SolventStabilizers.pdf.

[10] R.H. Bowman, P. Miller, M. Purchase, R. Schoellerman, Ozone-peroxide Advanced Oxidation Water Treatment System for Treatment of Chlorinated Solvents and 1,4- dioxane, Proceedings of the American Chemical Society National Meeting, San Diego, April 3, 2001.

[11] C.D. Adams, P.A. Scanlan, N.D. Secrist, Oxidation and biodegradability enhancement of 1,4-dioxane using hydrogen peroxide and ozone, Environ. Sci. Technol., 28 (1994) 1812–1818.

[12] M.M. Odah, R. Powell, D.J. Riddle, ART in-well technology proves effective in treating 1,4-dioxane contamination, Rem. J., 15 (2005) 51–64.

[13] M.I. Stefan, J.R. Bolton, Mechanism of the degradation of 1,4-dioxane in dilute aqueous solutions using the UV/hydrogen peroxide process, Environ. Sci. Technol., 32 (1998) 1588–1595.

[14] B.K. Min, J.E. Heo, N.K. Youn, O.S. Joo, H. Lee, J.H. Kim, H.S. Kim, Tuning of the photocatalytic 1,4-dioxane degradation with surface plasmon resonance of gold nanoparticles on titania, Cat. Comm., 10 (2009) 712–715.

[15] T. Vescovi, H. Coleman, R. Amal, The effect of pH on UV-based advanced oxidation technologies - 1,4-dioxane degradation, J. Hazard. Mater., 182 (2010) 75–79.

[16] W.J. Weber, E.J. Le Boeuf, Process for advanced treatment of water, Water Sci. Technol., 40 (1999) 11–19.

[17] P. Bose, W.H. Glaze, D.S. Maddox, Degradation of various advanced oxidation processes: 1. Reaction rates, Water Res., 32 (1998) 997–1004.

[18] A. Hirvonen, T. Tuhkanen, M. Ettala, S. Korhonen, P. Kalliokoski, Evaluation of a field-scale UV/H_2O_2 oxidation system for the purification of groundwater contaminated with PCE, Environ. Technol., 19 (1998) 821–828.

[19] S.M. Sock, A Comprehensive Evaluation of Biodegradation as a Treatment Alternative for the Removal of 1,4-Dioxane, MSc thesis, Clemson University, Clemson SC, 1993.

[20] M.J. Zenker, R.C. Borden, M.A. Barlas, Biodegradation of 1,4- dioxane using trickling filter, J. Environ. Eng., 130 (2003) 926–931.

[21] R.E. Parales, J.E. Adamus, N. White, H.D. May, Degradation of 1,4-dioxane by an *actinomycete* in pure culture, Appl. Environ. Microbiol., 60 (1994) 4527–4230.

[22] B.L. Burback, J.J. Perry, Biodegradation and biotransformation of groundwater pollutant mixtures by *Mycobacterium vaccae*, Appl. Environ. Microbiol., 59 (1993) 1025–1029.

[23] D. Bernhardt, H. Diekmann, Degradation of dioxane, tetrahydrofuran and other cyclic ethers by an environmental *Rhodococcus strain*, Appl. Microbiol. Biotechnol., 36 (1991) 120–123.

[24] M.J. Zenker, R.C. Borden, M.A. Barlaz, Mineralization of 1,4-dioxane in the presence of a structural analog, Biodegradation, 11 (2000) 239–246.

[25] S. Vainberg, K. McClay, H. Masuda, D. Root, C.W. Condee, G.J. Zylstra, R.J. Steffan, Biodegradation of ether pollutants by *Pseudonocardia* sp. *strain ENV478*, Appl. Environ. Microbiol., 72 (2006) 5218–5224.

[26] S. Mahendra, A. Grostern, L. Alvarez-Cohen, The impact of chlorinated solvent co-contaminants on the biodegradation kinetics of 1,4-dioxane, Chemosphere, 91 (2013) 88–92.

[27] J.S. Han, M.H. So, C.G. Kim, Optimization of biological wastewater treatment conditions for 1,4-dioxane decomposition in polyester manufacturing process, Water Sci. Technol., 59 (2009) 995–1002.

[28] DoD SERDP, Evaluation of branched hydrocarbons as stimulants for in situ cometabolic biodegradation of 1,4-dioxane and its associated co-contaminants, 2013b ER-2303. Avalable at: www.serdp.org/Program-Areas/Environmental-Restoration/

Contaminated-Groundwater/Emerging-Issues/ER-2303/ER-2303.

[29] Y.J. An, E.R. Carraway, PAH degradation by UV/H_2O_2 in per fluorinated surfactant solutions, Water Res., 36 (2002) 309–314.

[30] H.M. Coleman, V. Vimonses, C. Leslie, R. Amal, Degradation of 1,4-dioxane in water using TiO_2 based photocatalytic and H_2O_2/UV processes, J. Hazard. Mater., 146 (2007) 496–501.

[31] P. Ghosh, A.N. Samanta, S. Ray, Oxidation kinetics of degradation of 1,4-dioxane in aqueous solution by H_2O_2/Fe(II) system, J. Environ. Sci. Health, Part A, 45 (2010) 395–399.

[32] S. Nakagawa, Y. Kenmochi, K. Tutumi, T. Tanaka, I. Hirasawa, A study on the degradation of endocrine disruptors and dioxins by ozonation and advanced oxidation processes, J. Chem. Eng. Jpn., 35 (2002) 840–847.

[33] M. Pera-Titus, V. Garcia-Molina, M.A. Banos, J. Gimenez, S. Esplugas, Degradation of chlorophenols by means of advanced oxidation processes: a general review, Appl. Catal., B, 47 (2004) 219–256.

[34] S.C. Kwon, J.Y. Kim, S.M. Yoon, W. Bae, K.S. Kang, Y.W. Rhee, Treatment characteristic of 1,4-dioxane by ozone-based advanced oxidation processes, J. Ind. Eng. Chem., 18 (2012) 1951–1955.

[35] M.J. Zenker, R.C. Borden, M.A. Barlaz, Occurrence and treatment of 1, 4- dioxane in aqueous environments, J. Environ. Eng. Sci., 20 (2003) 423–432.

[36] N. Merayo, D. Hermosilla, L. Cortijo, Á. Blanco, Optimization of the Fenton treatment of 1,4-dioxane and on-line FTIR monitoring of the reaction, J. Hazard. Mater., 268 (2014) 102–109.

[37] M.A. Beckett, I. Hua, Enhanced sonochemical decomposition of 1,4-dioxane by ferrous iron, Water Res., 37 (2003) 2372.

[38] J. Carey, J. Lawrence, H. Tosine, Photodechlorination of PCB's in the presence of titanium dioxide in aqueous suspensions, Bull. Environ. Contam. Toxicol., 16 (1976) 697–701.

[39] Y. Ohko, D.A. Tryk, K. Hashimoto, A. Fujishima, Autoxidation of acetaldehyde initiated by TiO_2 photocatalysis under weak UV illumination, J. Phys. Chem. B, 102 (1998) 2699–2704.

[40] A. Fujishima, X. Zhang, D. Tryk, TiO_2 photocatalysis and related surface phenomena, Surf. Sci. Rep., 63 (2008) 515–582.

[41] H.S. Son, J.K. Im, K.D. Zoh. A, Fenton-like degradation mechanism for 1,4-dioxane using zero-valent iron (Fe^0) and UV light, Water Res., 43 (2009) 1457–1463.

[42] H. Barndõk, L. Cortijo, D. Hermosilla, C. Negro, Á. Blanco, Removal of 1,4-dioxane from industrial wastewaters: routes of decomposition under different operational conditions to determine the ozone oxidation capacity, J. Hazard. Mater., 280 (2014) 340–347.

[43] H. Barndõk, N. Merayo, L. Blanco, D. Hermosilla, Á. Blanco, Application of on-line FTIR methodology to study the mechanisms of heterogeneous advanced oxidation processes, Appl. Catal., B, 185 (2016) 344–352.

[44] H. Barndõk, D. Hermosilla, C. Han, D. Dionysiou, C. Negro, Á. Blanco, Degradation of 1,4-dioxane from industrial wastewater by solar photocatalysis using immobilized NF-TiO_2 composite with monodisperse TiO_2 nanoparticles, Appl. Catal., B, 180 (2016) 44–52.

[45] J.R. Alvarez-Corena, J.A. Bergendahl, F.L. Hart, Advanced oxidation of five contaminants in water by UV/TiO_2: reaction kinetics and byproducts identification, J. Environ. Manage., 181 (2016) 544–551.

[46] R.R. Hill, G.E. Jeffs, D.R. Roberts, Photocatalytic degradation of 1,4-dioxane in aqueous solution, J. Photochem. Photobiol. A, 108 (1997) 55–58.

[47] B.K. Min, J.E. Heo, N.K. Youn, O.S. Joo, H. Lee, J.H. Kim, H.S. Kim, Tuning of the photocatalytic 1,4-dioxane degradation with surface plasm on resonance of gold nanoparticles on titania, Catal. Commun., 10 (2009) 712–715.

[48] A. Nakajima, S. Matsui, S. Yanagida, Y. Kameshima, K. Okada, Preparation and properties of titania-Cs2.5H0.5PW12O40 hybrid films, Surf. Coat. Technol., 203 (2009) 1133–1137.

[49] R.P. Schwarzenbach, P.M. Gschwend, D.M. Imboden, Sorption, Solid-Aqueous Solution Exchange, in Environmental Organic Chemistry, John Wiley & Sons Inc., New York, 1993.

[50] C.E. Wayne, R.P. Wayne, Determination of Chloramphenicol in Tablets by Electrogenerated Chemiluminescence, In Photochemistry, Oxford University Press Inc., New York, 2002.

[51] A.J. Bard, R. Parsons, J. Jordan, Standard Potentials in Aqueous Solutions, International Union of Pure and Applied Chemistry, Marcel Dekker Inc., New York, 1985.

[52] W.H. Glaze, J.W. Kang, D.H. Chapin, The chemistry of water treatment processes involving ozone, hydrogen peroxide and ultraviolet radiation, Ozone Sci. Eng., 9 (1987) 335–352.

[53] G. Bertanza, M. Papa, R. Pedrazzani, C. Repice, G. Mazzoleni, N. Steimberg, D. Feretti, E. Ceretti, I. Zerbini, EDCs, estrogenicity and genotoxicity reduction in a mixed (domestic + textile) secondary effluent by means of ozonation: a full-scale experience, Sci. Total Environ., 458–460 (2013) 160–168.

[54] A.M. Deegan, B. Shaik, K. Nolan, K. Urell, M. Oelgemoeller, J. Tobin, A. Morrissey, Treatment options for wastewater effluents from pharmaceutical companies, Int. J. Environ. Sci. Technol., 8 (2011) 649–666.

[55] T.A. Larsen, J. Lienert, A. Joss, H. Siegrist, How to avoid pharmaceuticals in the aquatic environment, J. Biotechnol., 113 (2004) 295–304.

[56] I. Oller, S. Malato, J.A. Sanchez-Perez, Combination of advanced oxidation processes and biological treatments for wastewater decontamination-a review, Sci. Total Environ., 409 (2011) 4141–4166.

[57] J.H. Suh, M. Mohseni, A study on the relationship between biodegradability enhancement and oxidation of 1,4-dioxane using ozone and hydrogen peroxide, Water Res., 38 (2004) 2596–2604.

[58] J.L. Acero, S.B. Haderlein, T.C. Schmidt, M.J.F. Suter, U. Von Gunten, MTBE oxidation by conventional ozonation and the combination ozone/hydrogen peroxide: efficiency of the processes and bromate formation, Environ. Sci. Technol., 35 (2001) 4252–4259.

[59] F. Beltran, B. Acedo, J. Rivas, Use of ozone to remove alachlor from surface water, Bull. Environ. Contam. Toxicol., 62 (1999) 324–329.

[60] K. Ikehata, M.G. El-Din, Aqueous pesticide degradation by ozonation and ozone based advanced oxidation processes: a review (Part I), Ozone Sci. Eng., 27 (2005) 83–114.

[61] K. Ikehata, M.G. El-Din, Aqueous pesticide degradation by ozonation and ozone based advanced oxidation processes: a review (Part II), Ozone Sci. Eng., 27 (2005) 173–202.

[62] J. Hoigne, H. Bader, The role of hydroxyl radical reactions in ozonation processes in aqueous, Water Res., 10 (1976) 377–386.

[63] J. Hoigne, H. Bader, Rate constants of reactions of ozone with organic and inorganic compounds in water II, Water Res., 17 (1983) 11.

[64] A.B. Ross, Selected Specific Rates of Reactions of Transients from Water in Aqueous Solution: III. Hydroxyl Radical and Perhydroxyl Radical and Their Radical Ions, U.S. Department of Commerce, National Bureau of Standards, Washington, 1977.

[65] L. Bijan, M. Mohseni, Integrated ozone and biotreatment of pulp mill effluent and changes in biodegradability and molecular weight distribution of organic compounds, Water Res., 39 (2005) 3763–3772.

[66] K. Kosaka, H. Yamada, S. Matsui, K. Shishida, The effects of the co-existing compounds on the decomposition of micropollutants using the ozone/hydrogen peroxide process, Water Sci. Technol., 42 (2000) 353–361.

[67] J.H. Suh, D.J. Kang, J. Do Park, H.S. Lee, A Study on the Catalytic Ozonation of 1,4-Dioxane, Proc. 9th Russian-Korean International Symposium on Science & Technology KORUS´2005, 2005, pp. 169–171.

[68] V. Maurino, P. Calza, C. Minero, E. Pelizzetti, M. Vincenti, Light-assisted 1,4- dioxane degradation, Chemosphere, 35 (1997) 2675–2688.

[69] E. Evgenidou, K. Fytianos, I. Poulios, Photocatalytic oxidation of dimethoate in aqueous solutions, J. Photochem. Photobiol., A, 175 (2005) 29–38.

[70] J. Prousek, Advanced oxidation processes for water treatment. Photochemical processes, Chem. Listy, 90 (1996) 307–315.

[71] S. Malato, J. Blanco, M.I. Maldonado, P. Fernandez-Ibanez, A. Campos, Optimizing solar photocatalytic mineralization of pesticides by adding inorganic oxidizing species; application to the recycling of pesticide containers, Appl. Catal., B, 28 (2000) 163–174.

[72] M.S. Tsao, W.K. Wilmarth, The aqueous chemistry of inorganic free radicals. I. The mechanism of the photolytic decomposition of aqueous persulfate ion and evidence regarding the sulfatehydroxyl radical interconversion equilibrium, J. Phys. Chem., 63 (1959) 346–352.

[73] M. Dor, Chimie des Oxydants au Traitment des Eaux., Lavoisier, Paris, 1989, p. 296.

[74] K.H. Choo, D.I. Chang, K.W. Park, M.H. Kim, Use of an integrated photocatalysis/hollow fiber microfiltration system for the removal of trichloroethylene in water, J. Hazard. Mater., 152 (2008) 183–190.

[75] H. Barndok, Advanced Oxidation Processes for the Treatment of Industrial Wastewaters Containing 1,4-Dioxane, Ph.D. Thesis, UNIVERSIDAD COMPLUTENSE DE MADRID, FACULTAD DE CIENCIAS QUÍMICAS, Departamento de Ingeniería Química, Spain, 2016.

[76] M.S. Lucas, J.A. Peres, G.L. Puma, Treatment of winery waste-water by ozone-based advanced oxidation processes (O_3, O_3/UV and O_3/UV/H_2O_2) in a pilot-scale bubble column reactor and process economics, Sep. Purif. Technol., 72 (2010) 235.

[77] N. Azbar, T. Yonar, K. Kestioglu, Comparison of various advanced oxidation processes and chemical treatment methods for COD and color removal from a polyester and acetate fiber dyeing effluent, Chemosphere, 55 (2004) 35.

[78] R.G. Parag, Treatment of wastewater streams containing phenolic compounds using hybrid techniques based on cavitation: a review of the current status and the way forward, Ultrason. Sonochem., 15 (2008) 1–15.

[79] I.A. Balcioglu, M. Otker, Treatment of pharmaceutical waste-water containing antibiotics by O_3 and O_3/H_2O_2 processes, Chemosphere, 50 (2003) 85.

[80] S. Esplugas, J. Gimenez, S. Contreras, E. Pascual, M. Rodriquez, Comparison of different advanced oxidation processes for phenol degradation, Water Res., 36 (2002) 1034.

[81] T.O. Kwon, B.B. Park, I.S. Moon, advanced oxidation process for the treatment of terephthalic acid wastewater using UV, H_2O_2 and O_3: organic and color removal studies, Korean Chem. Eng. Res., 45 (2007) 648.

[82] R.G. Ball, Soil and Water Remediation Method and Apparatus, US Patent No. 7,667,087," 7,667,087 B2, 2010.

[83] SERDP (Strategic Environmental Research and Development Program), In Situ Chemical Oxidation for Groundwater Remediation, Vol. 3. Springer, New York, NY, 2011,

[84] R.G. Ball, Chemical Oxidation Method and Compounds US, Patent No. 8,049,056," 8,049,056 B2, 2011.

[85] S.G. Huling, B.E. Pivetz, In-situ Chemical Oxidation. U.S. Environmental Protection Agency, Office of Research and Development, National Risk Management Research Laboratory, 2006.

[86] A. Tsitonaki, B. Petri, M. Crimi, H. Mosbæk, R.L. Siegrist, P.L. Bjerg, In situ chemical oxidation of contaminated soil and groundwater using persulfate, a review, Crit. Rev. Environ. Sci. Technol., 40 (2008) 55–91.

[87] P.A. Block, R.A. Brown, D. Robinson, Novel activation technologies for sodium persulfate in situ chemical oxidation. In: Proc. Fourth International Conference on the Remediation of Chlorinated and Recalcitrant Compound, pp. 1–8, Vol. 2004, Paper 2A-0.

[88] E.S. FMC, In-situ Chemical Oxidation with KlozurTM Activated Persulfate: Comingled Plume of Chlorinated Solvents and 1,4 Dioxane. FMC Environmental Solutions, 2007.

[89] G. Cronk, Case Study: Comparison of Multiple Activation Methods for Sodium Persulfate Isco Treatment, In: Proc. Sixth International Conference on Remediation of Chlorinated and Recalcitrant Compounds, 2008.

[90] M.D. Paul, A.W. Barbara, K.M. Kelly, B. James, Fast-track Remedial Design of Full-scale ISCO Application Using Pilot Scale Testing and Field Screening Parameters, Proc. Annual International Conference on Soils, Sediments, Water and Energy, Vol. 15, 2010.

[91] D. Eberle, R. Ball, T.B. Boving, Peroxone activated persulfate treatment of 1,4-dioxane in the presence of chlorinated solvent co-contaminants, Chemosphere, 144 (2016) 728–735.

[92] F. Harber, J.J. Weiss, The catalytic decomposition of hydrogen peroxide by iron salts, J. Am. Chem. Soc., 45 (1934) 338–351.

[93] J.J. Pignatello, E. Oliveros, A. MacKay, Advanced oxidation processes for organic contaminant destruction based on the Fenton reaction and related chemistry, Crit. Rev. Environ. Sci. Technol., 36 (2006) 1–84.

[94] D. Hermosilla, M. Cortijo, C.P. Huang, The role of iron on the degradation and mineralization of organic compounds using conventional Fenton and photo- Fenton processes, Chem. Eng. J., 155 (2009) 637–646.

[95] R.F.F. Pontes, J.E.F. Moraes, A. Machulek Jr., J.M. Pinto, A mechanistic kinetic model for phenol degradation by the Fenton process, J. Hazard. Mater., 176 (2010) 402–413.

[96] J. Kiwi, C. Pulgarin, P. Peringer, M. Gratzel, Beneficial-effects of homogeneous photo-Fenton pretreatment upon the biodegradation of anthraquinone sulfonate in waste-water treatment, Appl. Catal., B, 3 (1993) 85–99.

[97] C. Pulgarin, J. Kiwi, Overview on photocatalytic and electro-catalytic pretreatment of industrial non-biodegradable pollutants and pesticides, Chimia, 50 (1996) 50–55.

[98] H.S. Kim, B.H. Kwon, S.J. Yoa, I.K. Kim, Degradation of 1,4-dioxane by photo- Fenton processes, J. Chem. Eng. Jpn., 41 (2008) 829–835.

[99] E. Khan, W. Wirojanagud, N. Sermsai, Effects of iron type in Fenton reaction on mineralization and biodegradability enhancement of hazardous organic compounds, J. Hazard. Mater., 161 (2009) 1024–1034.

[100] E. De Torres-Socias, I. Fernandez-Calderero, I. Oller, M.J. Trinidad-Lozano, F.J. Yuste, S. Malato, Cork boiling waste-water treatment at pilot plant scale: comparison of solar photo-Fenton and ozone (O_3, O_3/H_2O_2). Toxicity and biodegradability assessment, Chem. Eng. J., 234 (2013) 232–239.

[101] C. Mendoza-Marin, P. Osorio, N. Benitez, Decontamination of industrial wastewater from sugarcane crops by combining solar photo-Fenton and biological treatments, J. Hazard. Mater., 177 (2010) 851–855.

[102] I. Oller, S. Malato, J.A. Sanchez-Perez, M.I. Maldonado, W. Gernjak, L.A. Perez- Estrada, J.A. Munoz, C. Ramos, C. Pulgarin, Pre-industrial-scale combined solar photo-fenton and immobilized biomass activated-sludge biotreatment, Ind. Eng. Chem. Res., 46 (2007) 7467–7475.

[103] T.F.C.V. Silva, A. Fonseca, I. Saraiva, V.J.P. Vilar, R.A.R. Boa-ventura, Biodegradability enhancement of a leachate after biological lagooning using a solar driven photo-Fenton reaction, and further combination with an activated sludge biological process, at pre-industrial scale, Water Res., 47 (2013) 3543–3557.

[104] P.A. Soares, T.F.C.V. Silva, D.R. Manenti, S.M.A.G.U. Souza, R.A.R. Boaventura, V.J.P. Vilar, Insights into real cotton-textile dyeing wastewater treatment using solar advanced oxidation processes, Environ. Sci. Pollut. Res., 21 (2014) 932–945.

[105] B.S. Souza, F.C. Moreira, M.W.C. Dezotti, V.J.P. Vilar, R.A.R. Boaventura, Application of biological oxidation and solar driven advanced oxidation processes to remediation of winery wastewater, Catal. Today, 209 (2013) 201–208.

[106] V. Ragaini, E. Selli, C. Letizia, B.C. Pirola, Sono-photocatalytic degradation of 2-chlorophenol in water: kinetic and energetic comparison with other techniques, Ultrason. Sonochem., 8 (2001) 251–258.

[107] I.Z. Shirgaonkar, A.B. Pandi, Sonophotochemical destruction of aqueous solution of 2,4,6-trichlorophenol, Ultrason. Sonochem., 5 (1998) 53–61.

[108] Y. Kado, M. Atobe, T. Nonaka, Ultrasonic effects on electro organic processes ± Part 20. Photocatalytic oxidation of aliphatic alcohols in aqueous suspension of TiO2 powder, Ultrason. Sonochem., 8 (2001) 69–74.

[109] G.M. Klecˇka, S.J. Gonsior, Removal of 1,4-dioxane from wastewater, J. Hazard. Mater., 13 (1986) 161–168.

[110] S. Chitra, K. Paramasivan, M. Cheralathan, P.K. Sinha, Degradation of 1,4- dioxane using advanced oxidation processes, Environ. Sci. Pollut. Res., 19 (2012) 871–878.

[111] J. Maekawa, K. Mae, H. Nakagawa, Degradation of 1,4-dioxane by the ferrioxalate-mediated photo-Fenton process using UV or white LED irradiation, J. Chem. Eng. Jpn., 49 (2016) 305–311.

[112] E. Brillas, I. Sires, M.A. Oturan, Electro-Fenton process and related electrochemical technologies based on Fenton's reaction chemistry, Chem. Rev., 109 (2009) 6570–6631.

[113] O. Ganzenko, D. Huguenot, E.D. van Hullebusch, G. Esposito, M.A. Oturan, Electrochemical advanced oxidation and biological processes for wastewater treatment: a review of the combined approaches, Environ. Sci. Pollut. Res., 21 (2014) 8493–8524.

[114] P.V. Nidheesh, R. Gandhimathi, Trends in electro-Fenton process for water and wastewater treatment: an overview, Desalination, 299 (2012) 1–15.

[115] J. Antoni, M.C. Liu, P. Chewpreecha, Kinetics of aniline degradation by Fenton and electro-Fenton processes, Water Res., 40 (2006) 1841–1847.

[116] Y.H. Huang, Y.F. Huang, P.S. Chang, C.Y. Chen, Comparative study of oxidation of dye-Reactive Black B by different advanced oxidation processes: Fenton, electro-Fenton and photo-Fenton, J. Hazard. Mater., 154 (2008) 655–662.

[117] H. Nakagawa, S. Takagi, J. Maekawa, Fered-Fenton process for the degradation of 1,4-dioxane with an activated carbon electrode: a kinetic model including active radicals, Chem. Eng. J., 296 (2016) 398–405.

[118] R. Mantha, K.E. Taylor, N. Biswas, J.K. Bewtra, A continuous system for Fe⁰ reduction of nitrobenzene in synthetic wastewater, Environ. Sci. Technol., 35 (2001) 3231–3236.

[119] J.K. Moor, S.C Doney, D.M. Glover, I.Y. Fung, Iron cycling and nutrient-limitation patterns in surface waters of world ocean, Deep-Sea Res. II, 49 (2002) 493–507.

[120] W. Arnold, A.L. Roberts, Pathway and kinetics of chlorinated ethylene and chlorinated acetylene reaction with Fe⁰ particles, Environ. Sci. Technol., 34 (2000) 1794–1805.

[121] W.F. Wust, R. Kober, O. Schlicker, A. Dahmke, Combined zero- and first-order kinetic model of the degradation TCE and cis-DCE with commercial iron, Environ. Sci. Technol., 33 (1999) 4304–4309.

[122] B.H.J. Bielski, D.E. Cabelli, R.L. Arudi, A.B. Ross, Reactivity of OH_2/O_2 radicals in aqueous solution, J. Phys. Chem. Ref. Data, 14 (1985) 1041–1100.

[123] M. Balmer, B. Sulzberger, Atrazine degradation in irradiated iron/oxalate systems: effect of pH and oxalate, Environ. Sci. Technol., 33 (1999) 2148–2424.

[124] J.S. Jeong, J.Y. Joon, pH effect on OH radical production in photo/ferrioxalate system, Water Res., 39 (2005) 2893–2900.

[125] M.R. Hoffmann, S.T. Martin, W. Choi, D.W. Bahnemann, Environmental applications of semiconductor photocatalysis, Chem. Rev., 95 (1995) 69.

[126] D.M. Blake, Bibliography of Work on the Heterogeneous Photocatalytic Removal of Hazardous Compounds from Water and Air, National Renewable Energy Laboratory, Golden, CO, 2000.

[127] A. Fujishima, T.N. Rao, D.A. Tryk, Titanium dioxide photocatalysis, J. Photochem. Photobiol., C, 1 (2000) 1.

[128] A. Nakajima, M. Tanaka, Y. Kameshima, K. Okada, Sono-photocatalytic destruction of 1,4-dioxane in aqueous systems by HF-treated TiO_2 powder, J. Photochem. Photobiol. A, 167 (2004) 75.

[129] M. Mehrvar, W.A. Anderson, M. Moo-Young, Comparison of the photoactivities of two commercial titanium dioxide powders in the degradation of 1,4-dioxane, Int. J. Photoenergy, 4 (2002) 141–146.

[130] A. Mills, S. LeHunte, An overview of semiconductor photocatalysis, J. Photochem. Photobiol. A, 108 (1997) 1.

[131] S. Yamazaki, T. Tanimura, A. Yoshida, K. Hori, Reaction mechanism of photocatalytic degradation of chlorinated ethylenes on porous TiO_2 pellets: Cl radical-initiated mechanism, J. Phys. Chem. A, 108 (2004) 5183.

[132] L.L. Costa Alexandre G.S. Prado, TiO_2 nanotubes as recyclable catalyst for efficient photocatalytic degradation of indigo carmine dye, J. Photochem. Photobiol. A, 201 (2009) 45–49.

[133] S. Padikkaparambil, B. Narayanan, Z. Yaakob, S. Viswanathan, S.M. Tasirin, Au/TiO_2 Reusable photocatalysts for dye degradation, Int. J. Photoenergy, (2013) 1–10, Article ID 752605.

[134] Y. Xie, C. Yuan, X. Li, Photosensitized and photocatalyzed degradation of azo dye using Lnn+-TiO_2 sol in aqueous solution under visible light irradiation, Mater. Sci. Eng. B, 117 (2005) 325–333.

[135] D. Beydoun, R. Amal, G.K.–C. Low, S. McEvoy, Novel photocatalyst: titania-coated magnetite. Activity and photo-dissolution, J. Phys. Chem. B, 104 (2000) 4387–4396.

[136] C. Han, R. Luque, D.D. Dionysiou, Facile preparation of controllable size monodisperse anatase titania nanoparticles, Chem. Commun., 48 (2012) 1860–1862.

[137] N. Miranda-Garcia, S. Suarez, B. Sanchez, J.M. Coronado, S. Malato, M. Ignacio Maldonado, Photocatalytic degradation of emerging contaminants in municipal wastewater treatment plant effluents using immobilized TiO_2 in a solar pilot plant, Appl. Catal., B, 103 (2011) 294–301.

[138] M. Pelaez, P. Falaras, V. Likodimos, A.G. Kontos, A.A. de la Cruz, K. O'Shea, D.D. Dionysiou, Synthesis, structural characterization and evaluation of sol–gel-based NF-TiO_2 films with visible light-photoactivation for the removal of microcystin-LR, Appl. Catal., B, 99 (2010) 378–387.

[139] C.D. Vecitis, T. Lesko, A.J. Colussi, M.R. Hoffmann, Sonolytic decomposition of aqueous bioxalate in the presence of ozone, J. Phys. Chem. A, 114 (2010) 4968–4980.

[140] K. Lekkerkerker-Teunissen, A.H. Knol, L.P. van Altena, C.J. Houtman, J. Verberk, J.C. van Dijk, Serial ozone/peroxide/low pressure UV treatment for synergistic and effective organic micropollutant conversion, Sep. Purif. Technol., 100 (2012) 22–29.

[141] G.G. Bessegato, J.C. Cardoso, B.F. da Silva, M.V.B. Zanoni, Combination of photoelectrocatalysis and ozonation: a novel and powerful approach applied in Acid Yellow 1 mineralization, Appl. Catal., B, 180 (2016) 161–168.

[142] N. Kishimoto, Y. Yasuda, H. Mizutani, Y. Ono, Applicability of ozonation combined with electrolysis to 1,4-dioxane removal from wastewater containing radical scavengers, Ozone-Sci. Eng., 29 (2007) 13–22.

[143] J.P. Pocostales, M.M. Sein, W. Knolle, C. von Sonntag, T.C. Schmidt, Degradation of Ozone-refractory organic phosphates in wastewater by ozone and ozone/ hydrogen peroxide (peroxone): the role of ozone consumption by dissolved organic matter, Environ. Sci. Technol., 44 (2010) 8248–8253.

[144] H. Wang, B. Bakheet, S. Yuan, X. Li, G. Yu, S. Murayama, Y. Wang, Kinetics and energy efficiency for the degradation of 1,4-dioxane by electro-peroxone process, J. Hazard. Mater., 294 (2015) 90–98.

[145] P. Frangos, H.J. Wang, W.H. Shen, G. Yu, S.B. Deng, J. Huang, B. Wang, Y.J. Wang, A novel photoelectro-peroxone process for the degradation and mineralization of substituted benzenes in water, Chem. Eng. J., 286 (2016) 239–248.

[146] C. von Sonntag, U. von Gunten, Chemistry of Ozone in Water and Wastewater Treatment. From basic Principles to Applications, IWA Publishing, 2012.

[147] O. Legrini, E. Oliveros, A.M. Braun, Photochemical processes for water treatment, Chem. Rev., 93 (1993) 671–698.

[148] W. Shen, Y. Wang, J. Zhan, B. Wang, J. Huang, S. Deng, G. Yu, Kinetics and operational parameters for 1,4-dioxane degradation by the photoelectro-peroxone process, Chem. Eng. J., 310 (2017) 249–258.

[149] K.-C. Lee, K.-H. Choo, Hybridization of TiO_2 photocatalysis with coagulation and flocculation for 1,4-dioxane removal in drinking water treatment, Chem. Eng. J., 231 (2013) 227–235.

[150] S.S. Chin, K. Chiang, A.G. Fane, The stability of polymeric membranes in a TiO_2 photocatalysis process, J. Membr. Sci., 275 (2006) 202–211.

[151] R. Molinari, M. Borgese, E. Drioli, L. Palmisano, M. Schiavello, Hybrid processes coupling photocatalysis and membranes

for degradation of organic pollutants in water, Catal. Today, 75 (2002) 77–85.

[152] G. Balasubramanian, D.D. Dionysiou, M.T. Suidan, I. Baudin, J.M. Laîn_e, Evaluating the activities of immobilized TiO$_2$ powder films for the photocatalytic degradation of organic contaminants in water, Appl. Catal., B. 47 (2004) 73–84.

[153] J. Fu, M. Ji, Z. Wang, L. Jin, D. An, A new submerged membrane photocatalysis reactor (SMPR) for fulvic acid removal using a nano-structured photocatalyst, J. Hazard. Mater., 131 (2006) 238–242.

[154] S. Mozia, Photocatalytic membrane reactors (PMRs) in water and wastewater treatment. a review, Sep. Purif. Technol., 73 (2010) 71–91.

[155] V.C. Sarasidis, S.I. Patsios, A.J. Karabelas, A hybrid photo-catalysis- ultrafiltration continuous process: the case of poly-saccharide degradation, Sep. Purif. Technol., 80 (2011) 73–80.

[156] K.-H. Choo, R. Tao, M.-J. Kim, Use of a photocatalytic membrane reactor for the removal of natural organic matter in water: effect of photoinduced desorption and ferrihydrite adsorption, J. Membr. Sci., 322 (2008) 368–374.

[157] P. Wang, A.G. Fane, T.T. Lim, Evaluation of a submerged membrane vis-LED photoreactor (sMPR) for carbamazepine degradation and TiO$_2$ separation, Chem. Eng. J., 215–216 (2013) 240–251.

[158] S.-A. Lee, K.-H. Choo, C.-H. Lee, H.-I. Lee, T. Hyeon, W. Choi, H.-H. Kwon, Use of ultrafiltration membranes for the separation of TiO$_2$ photocatalysts in drinking water treatment, Ind. Eng. Chem. Res., 40 (2001) 1712–1719.

[159] R. Goei, Z. Dong, T.-T. Lim, High-permeability pluronic-based TiO2 hybrid photocatalytic membrane with hierarchical porosity: fabrication, characterizations and performances, Chem. Eng. J., 228 (2013) 1030–1039.

[160] R. Goei, T.-T. Lim, Ag-decorated TiO$_2$ photocatalytic membrane with hierarchical architecture: photocatalytic and anti-bacterial activities, Water Res., 59 (2014) 207–218.

[161] S.K. Papageorgiou, F.K. Katsaros, E.P. Favvas, G.E. Romanos, C.P. Athanasekou, K.G. Beltsios, O.I. Tzialla, P. Falaras, Alginate fibers as photocatalyst immobilizing agents applied in hybrid photocatalytic/ultrafiltration water treatment processes, Water Res., 46 (2012) 1858–1872.

[162] A.D. Syafei, C.-F. Lin, C.-H. Wu, Removal of natural organic matter by ultrafiltration with TiO$_2$-coated membrane under UV irradiation, J. Colloid Interface Sci., 323 (2008) 112–119.

[163] T.-T. Lim, P.-S. Yap, M. Srinivasan, A.G. Fane, TiO$_2$/AC composites for synergistic adsorption-photocatalysis processes: present challenges and further developments for water treatment and reclamation, Crit. Rev. Environ. Sci. Technol., 41 (2011) 1173–1230.

[164] S. Mozia, M. Tomaszewska, A.W. Morawski, A new photo-catalytic membrane reactor (PMR) for removal of azo-dye Acid Red 18 from water, Appl. Catal., B, 59 (2005) 131–137.

[165] S. Mozia, M. Tomaszewska, A.W. Morawski, Removal of azo-dye Acid Red 18 in two hybrid membrane systems employing a photodegradation process, Desalination, 198 (2006) 183–190.

[166] K.-C. Lee, H.-J. Beak, K.-H. Choo, Membrane photoreactor treatment of 1,4-dioxane-containing textile wastewater effluent: performance, modeling, and fouling control, Water Res., 86 (2015) 58–65.

[167] R. Gómez, T.L, ó pez, E. Ortiz-Islas, J. Navarrete, E. Sánchez, F. Tzompantzi, X. Bokhimi, Effect of sulfation on the photoactivity of TiO$_2$ sol–gel derived catalysts, J. Mol. Catal., A Chem., 193 (2003) 217.

[168] X. Wang, J.C. Yu, Y. Hou, X. Fu, Three-dimensionally ordered mesoporous molecular-sieve films as solid superacid photo-catalysts, Adv. Mater., 17 (2005) 99.

[169] G. Col ó n, M.C. Hoidalgo, G. Munuera, I. Ferino, M.G. Cutru-fello, J.A. Navío, Cu-doped TiO$_2$ systems with improved photocatalytic activity, Appl. Catal., B 63 (2006) 45.

[170] R.-D. Sun, T. Nishikawa, A. Nakajima, T. Watanabe, K. Hashi-moto, TiO$_2$/polymer composite materials with reduced genera-tion of toxic chemicals during and after combustion—effect of HF-treated TiO$_2$, Polym. Degrad. Stab., 78 (2002) 479–484.

[171] S. Suzaki, T. Okazaki, Effect of surface fluorination on solid acidity and catalytic activity of TiO$_2$ and TiO$_2$-SiO$_2$, J. Chem. Soc. Jpn., 84 (1981) 330–335 (in Japanese).

[172] J.M. Pettibone, D.M. Cwiertny, M. Scherer, V.H. Grassian, Adsorption of organic acids on TiO$_2$ nanoparticles: effects of pH, nanoparticle size, and nanoparticle aggregation. Langmuir, 24 (2008) 6659–6667.

[173] V.K. Sharma, N.J.D. Graham, X.-Z. Li, B.-L. Yuan, Ferrate (VI) enhanced photocatalytic oxidation of pollutants in aqueous TiO$_2$ suspensions, Environ. Sci. Pollut. Res., 17 (2010) 453–461.

[174] M. Mehrvar, W.A. Anderson, M. Moo-Young, Photocatalytic degradation of aqueous tetrahydrofuran, 1,4-dioxane, and their mixture with TiO$_2$, Int. J. Photoenergy, 2 (2000) 67–80.

[175] P. Ettireddy, G. Reddy, G. Smirniotis, Sonophotocatalytic destruction of organic contaminantsin aqueous systems on TiO2 powders, Appl. Catal., B, 32 (2001) 95–105.

[176] S. Sakthivel, N. Neppolian, M.V. Shankar, B. Arabindoo, M. Palanichamy, V. Murugesan, Solar photocatalytic degra-dation of azo dye: comparison of photocatalytic efficiency of ZnO and TiO$_2$, Sol. Energy Mater. Sol. Cells, 77 (2004) 65–82.

[177] R. Andreozzi, V. Caprio, A. Insola, R. Marotta, Advanced oxidation processes (AOP) for water purification and recovery, Catal. Today, 53 (1999) 51–59.

[178] M. Mehrvar, W.A. Anderson, M. Moo-Young, Photocatalytic degradation of aqueous organic solvents in the presence of hydroxyl radical scavengers, Int. J. Photoenergy, 3 (2001) 187–191.

[179] C.D. Adams, P.A. Scanlan, N.D. Secrist, Oxidation and biodegradability enhance-ment of 1,4-dioxane using hydro-gen peroxide and ozone, Environ. Sci. Technol., 28 (1994) 1812–1818.

[180] W.H. Glaze, Reaction products of ozone – a review, Environ. Health Persp., 69 (1986) 151–157.

[181] J. Staehelin, J. Hoigne, Decomposition of ozone in water – rate of initiation by hydroxide ions and hydrogen-peroxide, Environ. Sci. Technol., 16 (1982) 676–681.

[182] A. Fischbacher, J. von Sonntag, C. von Sonntag, T.C. Schmidt, The ·OH radical yield in the H$_2$O$_2$+ O$_3$(peroxone) reaction, Environ. Sci. Technol., 47 (2013) 9959–9964.

[183] M.M. Sein, A. Golloch, T.C. Schmidt, C. von Sonntag, No marked kinetic isotope effect in the peroxone (H$_2$O$_2$/D$_2$O$_2$+ O$_3$) reaction: mechanistic consequences, Chemphyschem, 8 (2007) 2065–2067.

[184] S.W. Lam, M. Hermawan, H.M. Coleman, K. Fisher, R. Amal, The role of copper(II) ions in the photocatalytic oxidation of 1,4-dioxane, J. Mol. Catal. A, 278 (2007) 152–159.

[185] H.S. Son, S.B. Choi, E. Khan, K.D. Zoh, Removal of 1,4-dioxane from water using sonication: effect of adding oxidants on the degradation kinetics, Water Res., 40 (2006) 692.

[186] R.J. Brandi, C.A. Martín, O.M. Alfano, A.E. Cassano, A laboratory reactor for photocatalytic studies in slurry operation, J. Adv. Oxid. Technol., 5 (2002) 175–185.

[187] C.N. Chang, Y.S. Ma, G.C. Fang, A.C. Chao, M.C. Tsai, H.F. Sung, Decolorizing of lignin wastewater using the photochemical UV/TiO$_2$ process, Chemosphere. 56 (2004) 1011–1017.

[188] N. Merayo, D. Hermosilla, L. Blanco, L. Cortijo, A. Blanco, Assessing the application of advanced oxidation processes, and their combination with biological treatment, to effluents from pulp and paper industry, J. Hazard. Mater., 262 (2013) 420–427.

[189] M.F. Kabir, E. Vaisman, C.H. Landford, A. Kantzas, Effects of hydrogen peroxide in a fluidized bed photocatalytic reactor for wastewater purification, Chem. Eng. J., 118 (2006) 207–212.

[190] I. Poulios, E. Micropoulou, R. Panou, E. Kostopoulou, Photooxidation of eosinYin the presence of semiconducting oxides, Appl. Catal., B, 41 (2003) 345–355.

[191] A.E.H. Machado, J.A. de Miranda, R.F. de Freitas, E.T.F.M. Duarte, L.F. Ferreira, Y.D.T. Albuquerque, R. Ruggeiro, C. Sattler, L. de Oliveria, Destruction of the organic matter present in effluent from a cellulose and paper industry using photocatalysis, J. Photochem. Photobiol., A, 155 (2003) 231–241.

[192] H.D. Chun, J.K. Park, Photocatalytic oxidation of chlorinated organic compounds over TiO$_2$ membrane coated on glass tube, J. Hazard. Mater., 11 (1994) 501–510.

[193] R. Dillert, I. Fornefett, U. Siebers, D. Bahnemann, Photocatalytic degradation of trinitrotoluene and trinitrobenzene: influence of hydrogen peroxide, J. Photochem. Photobiol., A, 94 (1996) 231–236.

[194] Y.J. Hong, Preparation and Characterization of Sol–Gel Derived Peroxo Titania and Its Application for Nano-Crystalline Dye Sensitized Solar Cell, Ph.D. thesis, University of New South Wales, Sydney, Australia, 2002.

[195] H. Yang, K. Zhang, R. Shi, X. Li, X. Dong, Y. Yu, Sol–gel synthesis of TiO$_2$ nanoparticles and photocatalytic degradation of methyl orange in aqueous TiO$_2$ suspensions, J. Alloys Compd., 413 (2006) 302–306.

[196] F. Haque, E. Vaisman, C.H. Langford, A. Kantzas, Preparation and performance of integrated photocatalyst adsorbent (IPCA) employed to degrade model organic compounds in synthetic wastewater, J. Photochem. Photobiol., A, 169 (2005) 21–27.

[197] K. Huang, R.A. Couttenye, G.E. Hoag, Kinetics of Heat-assisted Persulfate Oxidation of Methyl Tert-butyl Ether (MTBE), 49 (2002) 413–420.

[198] C. Liang, Z.S. Wang, C.J. Bruell, Influence of pH on persulfate oxidation of TCE at ambient temperatures, Chemosphere, 66 (2007) 106–113.

[199] S. Yanagida, A. Nakajima, Y. Kameshima, K. Okada, Effect of applying voltage on photocatalytic destruction of 1,4-dioxane in aqueous system, Catal. Commun., 7 (2006) 1042–1046.

[200] A. Tsuchida, T. Shimamura, S. Sawada, S. Sato, N. Serpone, S. Horikoshi, In-liquid Plasma. a stable light source for advanced oxidation processes in environmental remediation, Rad. Phys. Chem., 147 (2018) 53–58.

[201] C. Tang, V. Chen, The photocatalytic degradation of reactive black 5 using TiO$_2$/UV in an annular photoreactor, Water Res., 38 (2004) 2775–2781.

[202] P. Yao, K.H. Choo, M.H. Kim, A hybridized photocatalysis–microfiltration system with iron oxide-coated membranes for the removal of natural organic matter in water treatment: effects of iron oxide layers and colloids, Water Res., 43 (2009) 4238–4248.

[203] O.M. Alfano, D. Bahnemann, A.E. Cassano, R. Dillert, R. Goslich, Photocatalysis in water environments using artificial and solar light, Catal. Today, 58 (2000) 199–230.

[204] C.S. Zalazar, C.A. Martin, A.E. Cassano, Photocatalytic intrinsic reaction kinetics. II. Effects of oxygen concentration on the kinetics of the photocatalytic degradation of dichloroacetic acid, Chem. Eng. Sci., 60 (2005) 4311–4322.

[205] H. Kiang, X. Li, Y. Yang, K. Sze, Effects of dissolved oxygen, pH, and anions on the 2,3-dichlorophenol degradation by photocatalytic reaction with anodic TiO$_2$ nanotube films, Chemosphere, 73 (2008) 805–812.

[206] Y. Wang, C. Hong, TiO$_2$-mediated photomineralization of 2-chlorobiphenyl: the role of O$_2$, Water Res., 34 (2000) 2791–2797.

[207] H. Gerischer, A. Heller, The role of oxygen in photooxidation of organic molecules on semiconductor particles, J. Phys. Chem., 95 (1991) 5261–5267.

[208] N.K. Youn, J.E. Heo, O.S. Joo, H. Lee, J. Kim, B.K. Min, The effect of dissolved oxygen on the 1,4-dioxane degradation with TiO$_2$ and Au–TiO$_2$ photocatalysts, J. Hazard. Mater., 177 (2010) 216–221.

[209] S. Chavadej, P. Phuaphromyod, E. Gulari, P. Rangsunvigit, T. Sreethawong, Photocatalytic degradation of 2-propanol by using Pt/TiO$_2$ prepared by microemulsion technique, Chem. Eng. J., 137 (2008) 489–495.

[210] V. Iliev, D. Tomova, L. Bilyarska, A. Eliyas, L. Petrov, Photocatalytic properties of TiO$_2$ modified with platinum and silver nanoparticles in the degradation of oxalic acid in aqueous solution, Appl. Catal., B, 63 (2006) 266–271.

[211] Y. Ma, C. Chang, Y. Chiang, H. Sung, A.C. Chao, Photocatalytic degradation of lignin using Pt/TiO$_2$ as the catalyst, Chemosphere, 71 (2008) 998–1004.

[212] A. Dawson, P.V. Kamat, Semiconductor–metal nanocomposites. Photoinduced fusion and photocatalysis of gold-capped TiO$_2$ (TiO$_2$/gold) nanoparticles, J. Phys. Chem. B, 105 (2001) 960–966.

[213] V. Iliev, D. Tomova, L. Bilyarska, G. Tyuliev, Influence of the size of gold nanoparticles deposited on TiO$_2$ upon the photocatalytic destruction of oxalic acid, J. Mol. Catal. A, 263 (2007) 32–38.

[214] D. Chen, M. Sivakumar, K.A. Ray, Dev. Synthesis of nickel nanoparticles in water-in-oil microemulsions, Chem. Eng. Miner. Process, 8 (2000) 506.

[215] D.F. Ollis, Photocatalytic purification and remediation of contaminated air and water, Surf. Chem. Catal., 3 (2000) 407.

[216] S.W. Lam, K. Chiang, T.M. Lim, R. Amal, G.K.-C. Low, Effect of charge trapping species of cupric ions on the photocatalytic oxidation of resorcinol, Appl. Catal., B, 55 (2005) 123.

[217] D. Beydoun, H. Tse, R. Amal, G.K.-C. Low, S. McEvoy, Effect of copper(II) on the photocatalytic degradation of sucrose, J. Mol. Catal., A, 177 (2002) 265.

[218] E.C. Butler, A.P. Davis, Photocatalytic oxidation in aqueous titanium dioxide suspensions: the influence of dissolved transition metals, J. Photochem. Photobiol., A, 70 (1993) 273.

[219] K.-I. Okamoto, Y. Yamamoto, H. Tanaka, M. Tanaka, A. Itaya, Heterogeneous photocatalytic decomposition of phenol over TiO$_2$ powder, Bull. Chem. Soc. Jpn., 58 (1985) 2015.

[220] N. San, A. Hatipoglu, G. Kocturk, Z. Cinar, Photocatalytic degradation of 4-nitrophenol in aqueous TiO$_2$ suspensions: theoretical prediction of the intermediates, J. Photochem. Photobiol. A, 146 (2002) 189.

[221] V. Brezova, A. Blazkova, E. Borosova, M. Sepan, R. Fiala, The influence of dissolved metal ions on the photocatalytic degradation of phenol in aqueous TiO$_2$ suspensions, J. Mol. Catal. A, 98 (1995) 109.

[222] S.W. Lam, M. Hermawan, H.M. Coleman, K. Fisher, R. Amal. The role of copper (II) ions in the photocatalytic oxidation of 1,4-dioxane, J. Mol. Catal. A, 278 (2007) 152–159.

[223] W.J. Cooper, C.J. Cramer, N.H. Martin, S.P. Mezyk, K.E. O'Shea, C. vonSonntag, Free radical mechanisms for the treatment of methyl tert-butyl ether (MTBE) via advanced oxidation/reductive processes in aqueous solutions, Chem. Rev., 109 (2009) 1302–1345.

[224] C. von Sonntag, H.-P. Schuchmann, Peroxyl Radicals in Aqueous Solutions, in: Z. Alfassi, Ed., Peroxyl Radicals, John Wiley, New York, 1997, pp. 173–234.

[225] J.E. Bennett, R. Summers, Product studies of the mutual termination reactions of sec-alkylperoxy radicals: evidence for non-cyclic termination, Can. J. Chem., 52 (1974) 1377–1379.

[226] M.A. Beckett, I. Hua, Elucidation of the 1,4-dioxane decomposition pathway at discrete ultrasonic frequencies, Environ. Sci. Technol., 34 (2000) 3944–3953.

[227] D. Vasudevan, A.T. Stone, Adsorption of catechols, 2-amino-phenols, and 1,2-phenylenediamines at the metal (hydr)oxide/water interface: effect of ring substituents on the adsorption onto TiO$_2$, Environ. Sci. Technol., 30 (1996) 1604.

[228] N. Karpel Vel Leitner, M. Dore, Mechanism of the reaction between hydroxyl radicals and glycolic, glyoxylic, acetic and oxalic acids in aqueous solution: consequence on hydrogen peroxide consumption in the H$_2$O$_2$/UV and O$_3$/H$_2$O$_2$ Systems, Water Res., 31 (1997) 1383–1397.

[229] Y. Tan, Y.B. Lim, K.E. Altieri, S.P. Seitzinger, B.J. Turpin, Mechanisms leading to oligomers and SOA through aqueous photooxidation: insights from OH radical oxidation of acetic acid and methylglyoxal, Atmos. Chem. Phys., 12 (2012) 801–813.

[230] G.V. Buxton, C.L. Greenstock, W.P. Helman, A.B. Ross, Critical review of rate constants for reactions of hydrated electrons, hydrogen atoms and hydroxyl radicals ($^{\bullet}$OH/$^{\bullet}$O$^-$ in aqueous solution, J. Phys. Chem. Ref. Data, 17 (1988) 513–886.

[231] A. Abe, Distribution of 1,4-dioxane in relation to possible sources in the water environment, Sci. Total Environ. 227 (1999) 41–47.

[232] A.A. Safarzadeh, J.R. Bolton, S.R. Caster, Ferrioxalate-mediated photodegradation of organic pollutants in contaminated water, Water Res., 31 (1997) 787–798.

[233] E.L. Fincher, W.J. Payne, Bacterial utilization of ether glycols, Appl. Microbiol., 10 (1962) 542–547.

[234] F.J. Barajas-Rodriguez, L.C. Murdoch, R.W. Falta, D.L. Freedman, Simulation of in situ biodegradation of 1,4-dioxane under metabolic and cometabolic conditions, J. Contam. Hydrol., 223 (2019) 103464.

[235] S. Mahendra, L. Alvarez-Cohen, *Pseudonocardia dioxanivorans* sp. nov., a novel actinomycete that grows on 1,4-dioxane, Int. J. Syst. Evol. Microbiol., 55 (2005) 593–598.

[236] U. Kohlweyer, B. Thiemer, T. Schrader, J.R. Andreesen, Tetrahydrofuran degradation by a newly isolated culture of *Pseudonocardia* sp. strain K1, FEMS Microbiol. Lett., 186 (2000) 301–306.

[237] K. Nakamiya, S. Hashimoto, H. Ito, J.S. Edmonds, M. Morita, Degradation of 1,4-dioxane and cyclic ethers by an isolated fungus, Appl. Environ. Microbiol., 71 (2005) 1254–1258.

[238] S. Mahendra, L. Alvarez-Cohen, Kinetics of 1,4-Dioxane biodegradation by monooxygenase-expressing bacteria, Environ. Sci. Technol., 40 (2006) 5435–5442.

[239] K. Sei, K. Miyagaki, T. Kakinoki, K. Fukugasako, D. Inoue, M. Ike, Isolation and characterization of bacterial strains that have high ability to degrade 1,4-dioxane as a sole carbon and energy source, Biodegradation, 24 (2013) 665–674.

[240] S.R. Kane, A.Y. Chakicherla, P.S. Chain, R. Schmidt, M.W. Shin, T.C. Legler, K.M. Scow, F.W. Larimer, S.M. Lucas, P.M. Richardson, K.R. Hristova, Whole-genome analysis of the methyl tertiary-butyl ether-degrading beta-proteobacterium Methylibium petroleiphilum PM1, J. Bacteriol., 189 (2007) 1931–1945.

[241] B.L. Burback, J.J. Perry, Biodegradation and biotransformation of groundwater pollutant mixtures by *Mycobacterium vaccae*, Appl. Environ. Microbiol., 59 (1993) 1025–1029.

[242] N. Yamamoto, Y. Saito, D. Inoue, K. Sei, M. Ike, Characterization of newly isolated *Pseudonocardia* sp. N23 with high 1,4-dioxanedegrading ability, J. Biosci. Bioeng., 125 (2018) 552–558.

[243] Ministry of the Environment Government of Japan: Items Related to the Protection of Human Health. National Effluent Standards. Ministry of the Environment Government of Japan, Tokyo, 2012.

[244] Y. Kimura, K. Isaka, F. Kazama, Tolerance level of dissolved oxygen to feed into anaerobic ammonium oxidation (anammox) reactor, J. Water Environ. Technol., 9 (2011) 169–178.

[245] G. Cema, E. Płaza, J. Trela, J. Surmacz-Górska, Dissolved oxygen as a factor influencing nitrogen removal rates in a one-stage system with partial nitritation and Anammox process, Water Sci. Technol., 64 (2011) 1009–1015.

[246] K. Isaka, M. Udagawa, Y. Kimura, K. Sei, M. Ike, Biological wastewater treatment of 1,4-dioxane using polyethylene glycol gel carriers entrapping *Afipia* sp. D1, J. Biosci. Bioeng., 121 (2016) 203–208.

[247] A. Grostern, C.M. Sales, W.Q. Zhuang, O. Erbilgin, L. Alvarez-Cohen, Glyoxylate metabolism is a key feature of the metabolic degradation of 1,4-dioxane by *Pseudonocardia dioxanivorans* strain CB1190, Appl. Environ. Microbiol., 78 (2012) 3298–3308.

[248] D.Z. Chen, X.J. Jin, J. Chen, J.X. Ye, N.X. Jiang, J.M. Chen, Intermediates and substrate interaction of 1,4-dioxane degradation by the effective metabolizer *Xanthobacter flavus* DT8, Int. Biodeterior. Biodegrad., 106 (2016) 133–140.

[249] R.J. Steffan, K. McClay, S. Vainberg, C.W. Condee, D. Zhang, Biodegradation of the gasoline oxygenates methyl tert-butyl ether, ethyl tert-butyl ether, and tert-amyl methyl ether by propane-oxidizing bacteria, Appl. Environ. Microbiol., 63 (1997) 4216–4222.

[250] E.L. Johnson, C.A. Smith, K.T. O'Reilly, M.R. Hyman, Induction of methyl tertiary butyl ether (MTBE)-oxidizing activity in *Mycobacterium vaccae* JOB5 by MTBE, Appl. Environ. Microbiol,, 70 (2004) 1023–1030.

[251] D. Hunkeler, R.U. Meckenstock, B. Sherwood Lollar, T.C. Schmidt, J.T. Wilson, A Guide for Assessing Biodegradation and Source Identification of Organic Ground Water Contaminants Using Compound Specific Isotope Analysis (CSIA), US Environmental Protection Agency, Ada, Oklahoma, 2008.

[252] S.H.B. Wang, K.-H. Chu, Biodegradation of 1,4-dioxane: effects of enzyme inducers and trichloroethylene, Sci. Total Environ., 520 (2015) 154–159.

[253] K. Sei, K. Miyagaki, T. Kakinoki, K. Fukugasako, D. Inoue, M. Ike, Isolation and characterization of bacterial strains that have high ability to degrade 1,4-dioxane as a sole carbon and energy source, Biodegradation, 24 (2013) 665–674.

[254] K. Skinner, L. Cuiffetti, M. Hyman, Metabolism and cometabolism of cyclic ethers by a filamentous fungus, a *Graphium* sp., Appl. Environ. Microbiol., 75 (2009) 5514–5522.

[255] D.E. Burmaster, The new pollution: groundwater contamination, Environment, 24 (1982) 22–36.

[256] K. Nakamiya, S. Hashimoto, H. Ito, J.S. Edmonds, M. Morita, Degradation of 1,4-dioxane and cyclic ethers by an isolated fungus, Appl. Environ. Microbiol., 71 (2005) 1254–1258.

[257] R.L. Ely, K.J. Williamson, M.R. Hyman, D.J. Arp, Cometabolism of chlorinated solvents by nitrifying bacteria: kinetics, substrate interactions, toxicity effects, and bacterial response, Biotechnol. Bioeng., 54 (1997) 520–534.

[258] B. Sun, K. Ko, J.A. Ramsay, Biodegradation of 1,4-dioxane by a Flavobacterium, Biodegradation, 22 (2011) 651–659.

[259] J.D. Young, W.H. Braun, P.J. Gehring, B.S. Horvath, R.L Daniel, 1,4-Dioxane and ß-hydroxyethoxyacetic acid excretion in urine of humans exposed to dioxane vapors, Toxicol. Appl. Pharmacol., 38 (1976) 643–646.

[260] Y.-T. Woo, J.C. Arcos, M.F. Argus, G.W. Griffin, K. Nishiyama, Metabolism of dioxane: identification of -dioxane-2-one as the major urinary metabolite, Biochem. Pharmacol., 26 (1977) 1535–1538.

[261] K. Sei, T. Kakinoki, D. Inoue, S. Soda, M. Fujita, M. Ike, Evaluation of the biodegradation potential of 1,4-dioxane in river, soil and activated sludge samples, Biodegradation, 21 (2010) 585–591.

[262] S. Mahendra, C.J. Petzold, E.E. Baidoo, J.D. Keasling, L. Alvarez-Cohen, Identification of the intermediates of in vivo oxidation of 1,4- dioxane by monooxygenase-containing bacteria, Environ. Sci. Technol., 41 (2007) 7330 –7336.

[263] Y.-M. Kim, J.-R. Jeon, K. Murugesan, E.-J. Kim, Y.-S. Chang, Biodegradation of 1,4-dioxane and transformation of related cyclic compounds by a newly isolated Mycobacterium sp. PH-06, Biodegradation, 20 (2009) 511–519.

[264] S.-Y.D. Chiang, R. Mora, W.H. Diguiseppi, G. Davis, K. Sublette, P. Gedalanga, S. Mahendra, Characterizing the intrinsic bioremediation potential of 1,4-dioxane and trichloroethene using innovative environmental diagnostic tools, J. Environ. Monit., 14 (2012) 2317–2326.

[265] G.J. Zylstra, D.T. Gibson, Toluene degradation by *Pseudomonas putida* F1, J. Biol. Chem., 264 (1989) 14940–14946.

[266] J.O. Sharp, C.M. Sales, J.C. LeBlanc, J. Liu, T.K. Wood, L.D. Eltis, WW. Mohn, L. Alvarez-Cohen, An inducible propane monooxygenase is responsible for N-nitrosodimethylamine degradation by *Rhodococcus* sp. strain RHA1, Appl. Environ. Microbiol., 73 (2007) 6930–6938.

[267] P.B. Gedalanga, P. Pornwongthong, R. Mora, S-Y.D. Chiang, B. Baldwin, D. Ogles, S. Mahendra, Identification of biomarker genes to predict biodegradation of 1,4-dioxane, Appl. Environ. Microbiol., 80 (2014) 3209–3321.